Price Dynamics and Structural Breaks in Speculative Markets: A Case Study of Cryptocurrency

Omer Kara[†]

Latest Version

March 23, 2022

1st Draft

Abstract

This sutdy examines how the dynamic relationships between rival cryptocurrencies change over time and are affected by shocks. In particular, using a vector autoregressive model (VAR), Granger–causality test, and impulse response analysis, the price dynamics of Bitcoin, Litecoin, and Ripple are investigated by allowing multiple structural breaks. The data used in the analyses cover daily time–series observations over the period of April 2014-July 2018. Using the Qu and Perron (2007) methodology in a VAR shows that there are two strong structural breaks on November 12, 2015 and September 28, 2016. Thus, the data are split into three segments. The time–series analyses across segments suggest the following results: (1) the Granger–causality from the prices of other coins to Ripple price is gaining strength; (2) the response of each coin to a shock in Bitcoin price is same across segments; (3) in response to a shock in Litecoin price, the impact on Bitcoin price is decreasing over time but the effect on Ripple price is increasing; and (4) the impacts on Bitcoin and Litecoin prices are falling over time in response to a shock in Ripple price.

Keywords: Crytocurrency, Strcutural Breaks, VAR, IRF
JEL Classification Codes: C32, C51, G11, G17

I am grateful for the tireless advising and support given by my advisors Barry Goodwin, Jeffrey Prestemon, and Walter Thurman. All errors are my own. The latest version is available here. Please address correspondence to okara@ogu.edu.tr.

[†]Faculty Member, PhD in Department of Economics, Eskisehir Osmangazi University. E-mail: okara@ogu.edu.tr

Contents

List of Tables

List of Figures

1 Introduction

After the Great Recession had started due to the crash in the housing market, many individuals and companies lost money. At that time the majority of people openly distrusted the global financial system and were frustrated with the third–party institutions that charge high commissions on money transfers and keep a detailed record of transactions. In October 2008, a programmer under the pseudonym Satoshi Nakamoto[1] came up with a novel idea: a decentralized digital currency that can be transferred online via a peer–to–peer network with significantly lower transaction costs (Nakamoto, 2008). The decentralized feature of the currency allows its users to interact with one another anonymously and without third–party intervention. In essence, this feature is the Nakamoto's response to the global financial system as well as to the role of third–party institutions in mediating financial transactions. In January 2009, Satoshi launched the network and the first units of the digital currency, known as *Bitcoin*.

The Bitcoin network operates on the Bitcoin protocol, which is based on cryptographic methods and available as an open–source software. It allows users to store or transfer Bitcoins securely without an intermediary. In simple terms, users can transfer Bitcoins from computer to computer via a system of cryptographic hashes, and then keep them secure in a digital wallet with cryptographic digital signatures. Therefore, instead of relying on trusted third–party institutions, the Bitcoin network uses cryptographic proof to process transactions, verify the legitimacy of Bitcoins, and spread the verified transactions among the network.

Fundamentally, the Bitcoin network is a massive decentralized and fully distributed public ledger, called *blockchain*. Each Bitcoin transaction that has ever occurred since the beginning of the genesis block is recorded in the blockchain to prevent double–spending. The safety and integrity of the Bitcoin blockchain are maintained via a mining process that requires powerful computers to solve complicated algorithms. The mining process first helps to validate and timestamp transactions. Then, it adds transactions to the blockchain. A network member who performs the mining process is called miner. New Bitcoins are created digitally during the mining process and distributed to miners as a financial incentive, often called reward, for their effort to maintain the security and integrity of the blockchain. The amount of reward per block halves roughly every four years, called *halving*, to keep the number of Bitcoins within certain limits. The halving feature is essentially a part of the predictable and transparent monetary policy that governs the supply of Bitcoin.

As Bitcoin and the blockchain technology gained interest in the public domain, programmers utilized from the open–source Bitcoin protocol to create alternative digital currencies, called altcoins. These include coins created with better technology and security measures or developed for specific purposes or demographic groups. Due to the application of cryptographic methods, Bitcoin and altcoins are often referred to as cryptocurrency. In general terms, a cryptocurrency

[1]The identity of Satoshi remains unknown as of July 30, 2017, and it is not known whether Satoshi is a person or a group. See Chuen (2015), for the claims about the true identity of Satoshi.

is a digital currency designed to serve as a medium of exchange using cryptography for secure transactions. With the emergence and success of Bitcoin, cryptocurrencies have gained prominence in the public and media and shown an unprecedented growth over the last few years. As of July 2017, more than 980 cryptocurrencies exist with a total market capitalization of $89 billion.[2] Using the first mover advantage, Bitcoin is still the most popular and valuable cryptocurrency.

Cryptocurrencies are not used only for a medium of exchange. Similar to any other fiat currency, they are used as investment asset by individuals and financial institutions. However, due to the unregulated environment and extreme price volatility of cryptocurrencies, they are frequently used by speculators to generate easy money in a short time. Some studies have investigated the speculative behavior of Bitcoin and provide strong statistical evidence that Bitcoin contains a substantial speculative bubble component.[3] However, a comprehensive examination of historical Bitcoin prices shows that the extreme price fluctuations have often originated after some abrupt structural breaks, which may have risen in response to security breaches, government regulations, a reward halving, and even a darknet market involvement.

During the short history of Bitcoin, it experienced various extreme events. Bitcoin was released in January 2009, and until April 2010 there was no exchange or market for it. In May 2010, Laszlo Hanyecz made the first real–world transaction buying two pizzas in Jacksonville, Florida for 10, 000 Bitcoins. In June 2011, there was a massive security breach in MtGox, which was the most significant trading platform for Bitcoin at that time, and the Bitcoin price dropped from $32 to $2. Until August 2012, the price gradually increased to $15. With the beginning of 2013, a price rally started and continued until $266 in April 2013. In October 2013, the price dropped to $110 since FBI seized $28.5 million worth of Bitcoins from the accounts of a website called Silk Road, an online black market and the first darknet market best known as a platform for selling illegal drugs. After the Silk Road rumors ended, the price surged during the end of 2013 and reached to $1242. During 2014 and until the end of 2015, the Bitcoin price plunged to as low as $200 due to the bankruptcy of MtGox and a false report regarding Bitcoin ban in China. During May 2016, a hype started about the incoming halving, which was expected to occur in July 2016. Since then, the price has spiked to $2739 as of July 30, 2017. See `www.coindesk.com/price/` for historical Bitcoin prices.[4]

Recently, Bitcoin's prominence, extreme price volatility, and the essential features such as decentralized network and cryptographic security have grabbed the attention of researchers. In overall, most studies of Bitcoin have been carried out in four main areas: (1) the speculative behavior of the Bitcoin price; (2) the microeconomic and macroeconomic determinants of

[2]Figure 6 illustrates the course of the number of cryptocurrencies listed on `www.coinmarketcap.com` since April 28, 2013. The top twenty cryptocurrencies by market capitalization are presented in Table 19.

[3]See, among others, Malhotra and Maloo (2014), Ciaian et al. (2015), Bouoiyour and Selmi (2015), and Cheah and Fry (2015).

[4]As the Bitcoin prices have been surging recently, it is impossible to precisely show the structural breaks occurred during the relatively low price levels in a static figure. Thus, interested readers should visit `www.coindesk.com/price/` for historical bitcoin prices in an interactive figure.

the Bitcoin price; (3) cointegration relations among the Bitcoin prices in different exchange platforms; and (4) cointegration and dynamic relationships between the Bitcoin prices and some macroeconomic variables such as Dow Jones Industry Average, oil price, Federal Funds Rate, and gold price.[5] Although extensive research has been carried out on Bitcoin, there is only one study that has examined structural breaks in the Bitcoin prices. It is an astonishing gap in the literature considering the previously mentioned extreme events that may have caused structural breaks. Based on the Perron (1997) endogenous structural break test, Malhotra and Maloo (2014) provide evidence that the most significant breakpoint is in October 2013, which coincides with the crash in Bitcoin price after the Silk Road event.

In the cryptocurrency world, Bitcoin is often considered as a primary gateway that allows investors and speculators to enter various cryptocurrency markets and trade altcoins since the majority of the altcoins are traded only against Bitcoin. In essence, this fundamental connection creates an inherent relationship between the prices of Bitcoin and altcoins. An understanding of this relationship is of utmost importance for investors. However, in the literature, there is only one study that has investigated the price dependencies between various cryptocurrencies, especially Bitcoin and altcoins. It is a surprising gap considering the variety of altcoins and how their prices are related to the Bitcoin price. Using empirical and Gaussian copulas, Osterrieder et al. (2017) analyze correlations and tail dependencies among cryptocurrencies as well as their statistical properties. They provide statistical evidence that cryptocurrencies exhibit large tail dependencies, especially that share the same underlying technology.

Instead of focusing only on Bitcoin or examining the tail dependencies of various cryptocurrencies, this study diverges from the primary focus of the previous research and aims to fill the two gaps in the literature (i.e., structural break and inherent relationship between the prices of Bitcoin and altcoins). It seeks to understand how the dynamic relationships between rival cryptocurrencies change over time and are affected by shocks. In particular, the price dynamics of Bitcoin, Litecoin, and Ripple are investigated by allowing multiple structural breaks.[6] Understanding the price dynamics between these rival markets and how they change over time can help small investors to take trade positions in advance and reduce risks by hedging in highly speculative cryptocurrency markets.

In summary, the dynamics of these markets are investigated in three steps. In the first step, to choose a multi–equation time series model that fits the entire data, unit root and stationary tests are performed assuming no structural breaks. Then, a vector autoregressive model is constructed. In the second step, two structural breaks are endogenously estimated for the vector autoregressive model built in the first step using the Qu and Perron (2007) methodology.[7] In the third step, the data are split into three segments on the estimated break dates. Then, a vector autoregressive

[5]See, among other, Fink and Johann, 2014; Malhotra and Maloo, 2014; Ciaian et al., 2015; Georgoula et al., 2015; Kristoufek, 2015; Bouoiyour and Selmi, 2015; Cheah and Fry, 2015; Bouoiyour and Selmi, 2016; Wang et al., 2016; Zhu et al., 2017; Li and Wang, 2017.

[6]Figure 1 and Figure 2 display that prices in these markets move together since 2014.

[7]See Section 3 for the details of the Qu and Perron (2007) methodology.

model is carried out along with causality tests for each segment. Finally, impulse response analysis is performed to evaluate the nature of dynamic relations inherent in the estimates of the model for each segment.

The primary results of this study can be summarized as follows: (1) the application of Qu and Perron (2007) methodology in a vector autoregressive model concludes that there are two robust structural breaks in 11-12-2015 and 09-28-2016 (i.e., November 12, 2015 and September 28, 2016), which appear to have affected the price dynamics between the three rival cryptocurrencies; (2) the Granger–causality from the prices of other coins to Ripple price is gaining strength; (3) the response of each coin to a shock in Bitcoin price is same across segments; (4) in response to a shock in Litecoin price, the impact on Bitcoin price is decreasing over time but the effect on Ripple price is increasing; and (5) the impacts on Bitcoin and Litecoin prices are falling over time in response to a shock in Ripple price.

The paper proceeds as follows: Section 2 presents the relevant data sources; Section 3 presents the empirical methods; Section 5 provides the results of structural break tests using the entire data as well as the estimation and results for each segment; Section 6 discusses the results; and Section 7 concludes.

2 Data Descriptions

The analyses of this study are conducted with a daily dataset collected by BraveNewCoin (2017) and distributed by Quandl (2017). Table 1 presents the descriptive summary of data along with the sources and number of observations in the raw data. The data consist of historical global price indices for cryptocurrencies based on volume–weighted average prices from multiple exchanges. Specifically, BraveNewCoin (2017) calculates a global price index for each cryptocurrency every day. It is based on data aggregated from all exchanges[8] trading in that cryptocurrency for any other form of currency. For each currency market, a volume–weighted average is obtained from the latest price reported from each exchange. To derive the index, each value is converted to US dollars using current international fiat conversion rates and an overall volume–weighted average price is calculated based on the total volume in each market. BraveNewCoin (2017)'s data represents the cleanest and the most comprehensive cryptocurrency data with extensive history.

The BraveNewCoin (2017)'s data is downloaded from its starting date, 04-01-2014, until 07-29-2017. In order to analyze the price dynamics between rival cryptocurrencies, this study uses three out of the four largest coins in terms of the market capitalization as of July 30, 2017. The selected cryptocurrencies are Bitcoin, Litecoin, and Ripple. An important note is that the decision to analyze only three coins is taken since the scope of this research would have been too broad if there would have been an analysis of all cryptocurrencies. Bitcoin is selected since

[8]BraveNewCoin (2017) surveys more than a hundred trading platforms for cryptocurrency/fiat trading pairs.

it is the coin that started the whole cryptocurrency era, and also it is still the most used and popular cryptocurrency. Litecoin and Ripple are particularly selected since they have existed on the starting date of the BraveNewCoin (2017)'s data, which ensures that there are sufficiently long data to analyze the price dynamics. Out of the top four cryptocurrencies, Ethereum is intentionally omitted due to its late release on July 30, 2015, compared to the selected coins.

The top twenty cryptocurrencies by market capitalization and monthly volume are presented in Table 19 and Table 20 respectively. Among the selected coins, Bitcoin is the most valuable coin traded at $2739.43 with a %50.43 market capitalization share as of July 30, 2017. Litecoin and Ripple are traded at $40.96 and $0.17 with a %2.39 and %7.13 market capitalization share respectively. Moreover, these coins are in the top five cryptocurrencies regarding monthly volume. In total, the selected cryptocurrencies represent %59.95 and %45.93 of the market capitalization and monthly volume share as of July 30, 2017. Figure 7 and Figure 8 can be exploited to compare the selected coins and all other coins in terms of market capitalization over time. These figures show that the selected coins have dominated the cryptocurrency market since 2013, regarding market capitalization. Similarly, comparing these coins regarding volume leads to the same conclusion as shown in Figure 9 and Figure 10.

Finally, all of the price series[9] are transformed into the rate of return form, and only the transformed forms are used for analyses. The main reason for this approach is the vast differences between the scale of coin prices. Adopting the rate of return form for each variable establishes a common scale for all price series. Table 2 presents the summary statistics of variables including the transformed forms. Figure 1 presents plots of all variables.[10] For easy comparison, all variables are plotted together in Figure 2.[11] The blue dotted lines indicate the estimated structural break dates (i.e., 11-12-2015 and 09-28-2016) using the Qu and Perron (2007) methodology. The red dotted line represents the 2nd halving of the Bitcoin blockchain, 07-09-2016.[12]

In order to prevent repetition, in the text, tables, and figures of the subsequent sections, a symbol is designated to the rate of return form of each series. These symbols are *BTC* for Bitcoin, *LTC* for Litecoin, and *XRP* for Ripple.

All analyses performed in this study, including the data downloading and cleaning parts, are completed using open source software R. Appendix A presents the R version information along with the used packages. GAUSS software is used only for estimating the multiple structural break dates with the Qu and Perron (2007) methodology. Appendix B presents the GAUSS version information.

[9]Throughout this study, *series*, *time series variable*, and *variable* are used interchangeably to refer to an individual time series in the data.

[10]Figure 11 presents plots for the same variables in the rate of return form.

[11]Figure 12 presents the plot for the same variables in the rate of return form.

[12]The 1st halving of the Bitcoin blockchain occurred in 11-28-2012.

3 Empirical Methods

This section presents the empirical methods performed on the entire data as well as on each segment after the data are split into three. The section proceeds as follows: Section 3.1 presents the unit root and stationary tests; Section 3.2 briefly summarizes the vector autoregressive model; and Section 3.3 through Section 3.5 cover the details of causality and model diagnostic tests as well as the impulse response analysis for interpreting the dynamics of the model.

3.1 Unit Root and Stationary Tests

Unit root testing of a time series variable is often the first step in time series analyses. If any of the variables in a time series regression has a unit root[13], then there might be a spurious regression problem as pointed out by Granger and Newbold (1974) and Phillips (1986). In order to avoid the spurious regression problem, a non–stationary process should be transformed into a stationary process. Detrending and differencing can help to stabilize the mean of a time series by eliminating trend and seasonality. Thus, these methods can yield a stationary process. However, the correct transformation method depends on whether the series is a trend–stationary process (TSP) or a difference–stationary process (DSP). A DSP should be differenced whereas a TSP should be detrended by regressing it on deterministic functions of time. Applying a wrong method might cause over or under differencing depending on the true data generating process (DGP) and result in specification error in time series regressions.

Before testing each series for unit root, it is better to investigate whether there is a seasonal unit root in the variable of interest. Two methods performed for testing seasonal unit root are Osborn–Chui–Smith–Birchenhall test by Osborn et al. (1988) and Canova–Hansen test by Canova and Hansen (1995).

A joint application of two groups of tests is conducted to test each series for unit root. In the first group, commonly used unit root tests are applied. These tests are Augmented Dickey–Fuller (ADF) unit root test by Dickey and Fuller (1979, 1981), Phillips–Perron (PP) unit root test by Phillips and Perron (1988), and Elliott–Rothenberg–Stock (ERS) unit root test by Elliott et al. (1996).[14] In the second group, Kwiatkowski–Phillips–Schmidt–Shin stationary test by Kwiatkowski et al. (1992) is performed.[15] This joint application is implemented as a confirmatory analysis such that a non–rejection in the first group of tests confirms a rejection in the second group of tests.

An important practical issue for the unit root and stationarity tests is the selection of the lag length p. If p is too small, then the remaining serial correlation in errors will bias the test

[13] In the time series literature, the following groups of concepts are used interchangeably: (1) *stationary* and *integrated order of zero* (i.e., $I(0)$); and (2) *unit root*, *non–stationary*, and *integrated order of one* (i.e., $I(1)$) assuming that the variable of interest has a single unit root.

[14] In ADF, PP, and ERS unit root tests, the null hypothesis is that *series is non–stationary*.

[15] In KPSS stationary test, the null hypothesis is that *series is stationary*.

whereas if p is too large, then the power of a test will suffer. Therefore, various lag length selection criteria are considered and employed in all tests.

The conventional unit root tests presented above require prior knowledge about the DGP. For instance, inappropriate exclusion of an intercept or a trend leads to biased coefficient estimates and causes size problems whereas inappropriate inclusion reduces the power of a test. Thus, these unit root tests work better when there is a priori knowledge about the DGP. Since the form of the DGP is entirely unknown to this study, Enders' ADF Procedure (EAP) by Enders (2004) is applied to reveal whether the variable of interest is a DSP or a TSP while testing for unit root as well. In summary, EAP performs several ADF unit root tests in a nested fashion. It starts with the least restrictive model (i.e., with intercept and trend) and proceeds sequentially until the most restrictive model (i.e., without any deterministic parts).[16]

For each series, EAP is performed with three lag length selection criteria which are Akaike Information Criterion (AIC), Bayesian Information Criterion (BIC), and Ng–Perron–Schwert (NPS).[17] The NPS is a backward lag length selection procedure performed in several steps: (1) define an upper bound, p_{max}, for the lag length p and set $p = p_{max}$, then use Schwert (1989)'s rule of thumb to determine the p_{max} with the integer of $12\sqrt[4]{N/100}$ value, where N is the length of a series; (2) estimate ADF unit root test regression with p; and (3) if $|\text{t-value}_{(p)}| > 1.6$, perform ADF unit root test with p; otherwise, reduce p by one and go back to the previous step.

PP unit root test is essentially a modification of ADF unit root test. It is based on a nonparametric correction to account for serial correlation. Although ADF and PP unit root tests are asymptotically equivalent, they might differ substantially in finite samples due to the different ways of correcting serial correlation. PP unit root test tends to be more powerful than ADF unit root test. On the other hand, PP unit root test is more sensitive to model misspecification, and it can have severe size distortions when autocorrelation of the error terms is negative. In this study, PP unit root test is performed under two models (i.e., a model with constant or trend) and with four lag lengths. Additional to AIC and BIC, two other methods are employed for selecting the lag length. These methods are commonly used in the literature and defined as *Long* and *Short* with the integer of $12\sqrt[4]{N/100}$ and $4\sqrt[4]{N/100}$ values respectively, where N is the length of a series.

ERS unit root test is another modification of ADF unit root test. It first detrends a time series with Generalized Least Squares and then applies ADF unit root test. ERS unit root test is considered as an efficient unit root test since it has substantially higher power than ADF and PP unit root tests especially when the root is close to unity and an unknown mean or trend is present. Elliott et al. (1996) show that it has the best overall performance concerning small–sample size and power. Thus, ERS unit root test is performed under two models and with four lag lengths as

[16]The whole procedure can be found in "Supplementary Manual to Accompany, Applied Econometric Time Series (4th Edition) by Walter Enders" at page 63-66 (see URL: `https://goo.gl/hd7uHN`) and in Enders (2004) at page 194-198.

[17]See Akaike (1974, 1998) for AIC, Schwarz et al. (1978) and Rissanen (1978) for BIC, and Schwert (1989) and Ng and Perron (2001) for NPS.

in the PP unit root test.

Power of ADF and PP unit root tests are low if the variable of interest is a stationary process with a root close to the non–stationary boundary. One way to get around the problem is to use a stationarity test such as KPSS stationary test. Thus, KPSS stationary test is performed under two models and with four lag lengths as in the PP and ERS unit root tests. In KPSS stationary test; however, *Long* and *Short* indicate the lag length decided with the integer of $10\sqrt{N}/14$ and $3\sqrt{N}/13$ values respectively, where N is the length of a series.

3.2 Vector Autoregressive Model

The Vector autoregressive model (VAR) was introduced by Sims (1980) as a technique to characterize the joint dynamic behavior among a set of variables. It has become a prevalent method of time series modeling since then.[18] VAR is often considered as an alternative to a large simultaneous equations model that does not account for the rich dynamic structure in time series data (Lütkepohl, 2006).

VAR typically treats all variables as a priori endogenous. Hence, it accounts for Sims' critique that the exogeneity assumptions for some variables in a simultaneous equations model are *ad hoc* and often not backed by fully developed theories. The only prior knowledge required in a VAR is a set of variables which can be hypothesized to affect each other intertemporally. Therefore, the estimation of VAR does not require as much information about the forces affecting a variable as do structural models with simultaneous equations. Based on this feature, Sims (1980) advocates the use of VAR as a theory–free method to estimate economic relationships.

VAR is a k-variable and k-equation linear model in which each variable is in turn explained by the lagged values of all variables and the error term. So, it is a multivariate version of a univariate autoregressive model with a single equation. The simple framework of VAR provides a systematic way to capture rich dynamics in multiple time series along with a statistical toolkit (e.g., impulse response analysis) that is easy to use and interpret.

A k-dimensional p^{th}-order VAR can be defined as

$$\mathbf{y_t} = \mathbf{c} + A_1\mathbf{y_{t-1}} + \cdots + A_p\mathbf{y_{t-p}} + \boldsymbol{\varepsilon_t} \tag{1}$$

where p is the lag length; T is the sample size; t indicates a temporal observation for $t = (1, \ldots, T)$; k is the number of endogenous time series variables and the total number of equations; $\mathbf{y_t} = (y_{1t}, \ldots, y_{kt})'$ is a $k \times 1$ vector for a set of k endogenous time series variables; $\mathbf{c} = (c_1, \ldots, c_k)'$ is a $k \times 1$ vector of constants allowing for the possibility of a nonzero mean $E(\mathbf{y_t})$; A_i's are $k \times k$ coefficient matrices for $i = (1, \ldots, p)$; and $\boldsymbol{\varepsilon_t} = (\varepsilon_{1t}, \ldots, \varepsilon_{kt})'$ is a $k \times 1$ vector of errors with zero mean white noise process and time invariant positive definite covariance matrix $E(\boldsymbol{\varepsilon_t}\boldsymbol{\varepsilon_t}') = \Sigma_\varepsilon$, that is $\boldsymbol{\varepsilon_t} \overset{iid}{\sim} (0, \Sigma_\varepsilon)$.[19] It is possible to add additional exogenous variables

[18] For a detailed literature review of VAR, see Watson (1994) and Lütkepohl (2005, 2011).

[19] Vectors are assigned by small bold letters and matrices by capital letters. Scalars are written out in small letters

(e.g., time trends and seasonal dummies) to any multiple–equation time series model. However, throughout this study, only the constant is included as an exogenous variable. The model in Eq. 1 is briefly called VAR(p) and can be estimated with standard ordinary least squares (OLS) and ML methods.

The process of choosing the lag length of VAR requires particular attention since coefficient inference, impulse response analysis and other formal tests depend on it. Choosing a lag length too small can lead to size distortions in formal tests whereas a too large lag length may imply reductions in power (Lütkepohl, 2005). Therefore, considering various lag lengths may provide useful insights. In the literature, information criteria such as AIC and BIC are often used for selecting the lag length of VAR. However, the present study considers only BIC for the lag length selection in all of the time series models and the related formal tests since AIC often estimates a lag length that is too large. For the VAR presented in Eq. 1, BIC is defined as

$$\mathrm{BIC}(p) = \ln \det \left(\hat{\Sigma}_\varepsilon(p) \right) + \frac{\ln T}{T} p k^2 \tag{2}$$

where $\hat{\Sigma}_\varepsilon(p) = T^{-1} \sum_{t=1}^{T} \hat{\boldsymbol{\varepsilon}}_\mathbf{t} \hat{\boldsymbol{\varepsilon}}_\mathbf{t}'$; and the other notations are as in Eq. 1.

Traditionally, VAR is designed for stationary variables. The underlying reason for this convention relates to one of the critical characteristics of VAR, that is, the stability of the model. VAR is stable if the following condition holds.

$$\det(I_k - A_1 z - \cdots - A_p z^p) \neq 0 \quad \text{for } |z| \leq 1 \tag{3}$$

where I_k is a $k \times k$ identity matrix; and the other notations are as in Eq. 1. The condition states that VAR is stable if the polynomial defined in Eq. 3 has no roots in and on the complex unit circle, which can be satisfied by having stationary variables only. Whereas, VAR is not stable, if the polynomial has a unit root (e.g., the determinant is zero for $z = 1$) due to some non–stationary variables in the model. Therefore, all variables have to be stationary to ensure the stability of VAR.

3.3 Granger–Causality Tests

The concept of Granger–causality was introduced by Granger (1969) and became quite popular in the time series literature due to its easy application in the context of VAR. According to Granger–causality, if a time series y_{1t} Granger–causes a time series y_{2t}, then the past values of y_{1t} should contain information that helps to predict y_{2t} above and beyond the information contained in the past values of y_{2t} alone. In a general sense, it is a statistical hypothesis test (e.g., through a series of F–tests on the lagged values of y_{1t} and y_{2t}) for determining whether the series y_{1t} is useful in forecasting y_{2t}.

which are possibly subscripted.

To test for Granger–causality between two stationary time series, consider a 2–dimensional version of VAR(p) presented in Eq. 1 and rewrite it with the matrix notation as follows:

$$\begin{bmatrix} y_{1t} \\ y_{2t} \end{bmatrix} = \begin{bmatrix} c_1 \\ c_2 \end{bmatrix} + \sum_{i=1}^{p} \begin{bmatrix} A_{11,i} & A_{12,i} \\ A_{21,i} & A_{22,i} \end{bmatrix} \begin{bmatrix} y_{1,t-i} \\ y_{2,t-i} \end{bmatrix} + \begin{bmatrix} \varepsilon_{1t} \\ \varepsilon_{2t} \end{bmatrix} \tag{4}$$

Then, y_{2t} does not Granger–cause y_{1t} if and only if the hypothesis

$$H_0 : A_{12,i} = 0 \quad \text{for} \quad i = 1, \ldots, p \tag{5}$$

is true. Similarly, y_{1t} does not Granger–cause y_{2t} if and only if the hypothesis

$$H_0 : A_{21,i} = 0 \quad \text{for} \quad i = 1, \ldots, p \tag{6}$$

is true. In each case, a rejection of the null hypothesis implies there is Granger–causality. A Wald test is a standard choice for testing the above hypotheses since a set of liner restrictions should be tested simultaneously. Under the null hypothesis, the Wald test statistic follows a usual asymptotic χ^2 distribution with p degrees of freedom.

3.4 Diagnostic Tests

Once a VAR is estimated, it is of central interest to test whether the residuals obey the model assumptions with a set of diagnostic tests. That is, one should check for the absence of autocorrelation and heteroskedasticity in the model residuals, and see whether the error process is normally distributed. Therefore, univariate and multivariate versions of formal tests for residual autocorrelation, conditional heteroskedasticity, and non–normality are conducted. The univariate diagnostic tests are applied to the residuals of the individual equations whereas the multivariate versions are used to diagnose the residual vector of VAR.

Ljung–Box (LB) test by Ljung and Box (1978) is a standard tool for checking autocorrelation of residuals in VAR.[20] The null hypothesis of LB test is that all of the residual autocovariances are zero (i.e., no serial correlation). LB test jointly examines the first h lags of serial correlation in residual. The choice of the lag length h is crucial for the small sample properties of the test. If h is chosen too low, then the approximation to the null distribution may be poor whereas a large h reduces the power of the test. In practice, the choice of h may affect the performance of the test. However, in the literature, there is little practical advice about how to choose h for LB test; and thus, using various h values is not uncommon in practice. Therefore, several h values are employed in all of the LB tests performed in this study. One condition for the multivariate LB test is that the h value should not be less than the lag length p in VAR(p). Therefore the following h values are selected for all of the LB tests: (1) the lag length p in VAR(p); (2) $\ln(T)$ which

[20]The univariate LB test has been generalized to the multivariate case by Hosking (1980, 1981) and Li and Mcleod (1981).

provides better power performance as suggested by some simulation studies (Tsay, 2005); (3) ten since it is indicated by Hyndman and Athanasopoulos (2014) conducting several simulation tests; (4) the frequency of the time series data; and (5) some other arbitrarily selected values.

For testing heteroskedasticity in the univariate and multivariate cases, the autoregressive conditional heteroskedasticity Lagrange multiplier (ARCH) test is performed (Engle, 1982; Hamilton, 1994; Lütkepohl, 2005). The null hypothesis of ARCH test is that there is no ARCH effect from lag 1 to lag h; and hence, residuals are homoskedastic. Conditional heteroskedasticity is often a concern for models based on time series data with monthly or higher frequency. Therefore, to investigate the ARCH effect in the model residuals, same h values used in the LB tests are employed.

Normality test is often used for model diagnosis although it is not a necessary condition for the validity of the statistical tests or estimators pertaining to VAR. However, non–normality of the residuals may indicate other model deficiencies such as non–linearities or structural change (Lütkepohl, 2011). Therefore, Jarque–Bera (JB) normality test by Jarque and Bera (1987) is applied to test for normality of the residuals in the univariate and multivariate cases. Moreover, separate tests for only skewness and only kurtosis is performed for each case.

3.5 Impulse Response Analysis

In VAR, coefficient estimates are rarely the focus of the analysis since their interpretation is often hard due to the multidimensional system. Therefore, following Sims (1980)'s seminal paper, it is often of interest to analyze the dynamic relationships among the variables via impulse response analysis. It explains how an external one–time shock affects the dynamic path of a set of variables in a system. These dynamic paths are defined by impulse response functions (IRFs). More specifically, IRF measures the *response* of a variable as a function of time to an *impulse* in another variable, holding all else constant.

Impulse response analysis is often performed in terms of the moving average (MA) representation. For instance, the MA representation of the k-dimensional stable VAR(p) presented in Eq. 1 is given as

$$\mathbf{y_t} = \mathbf{c} + \sum_{i=0}^{\infty} \Phi_i \boldsymbol{\varepsilon}_{\mathbf{t-i}} \tag{7}$$

where $\Phi_0 = I_k$; and Φ_i's are $k \times k$ matrices which contain the impulse responses. The Φ_s matrices can be computed recursively as

$$\Phi_s = \sum_{j=1}^{s} \Phi_{s-j} A_j \quad \text{for} \quad s = 1, 2, \ldots \tag{8}$$

where $A_j = 0$ for $j > p$; and s indicates the time ahead from the impulse[21]. The $(i, j)^{\text{th}}$

[21] In VAR, an impulse in a variable is induced through the residual vector $\boldsymbol{\varepsilon}_{\mathbf{t}} = (\varepsilon_{1t}, \ldots, \varepsilon_{kt})'$. For instance, a non–zero element of $\boldsymbol{\varepsilon}_{\mathbf{t}}$ yields an equal change in the associated left–hand side variable. Then, it induces further

coefficients of the matrix Φ_s is interpreted as the expected response of variable $y_{i,t+s}$ to a unit shock in variable y_{jt}. Thus, the matrix $\Phi_{ij,s} = \frac{\partial y_{i,t+s}}{\partial \varepsilon_{jt}}$ as a function of s is called the impulse response function. An important note is that if VAR is stable, then the IRFs should converge to zero as the time from the impulse s gets large, that is, the effect of an impulse is *transitory*. However, the impact of a one–time shock in VECM may lead to *permanent* changes in some or all of the variables, that is, it shifts the system to a new equilibrium (Lütkepohl and Reimers, 1992; Lütkepohl, 2005).

In order to evaluate the dynamic relationships among the variables of a model, the Generalized IRFs[22] are used with a 90% confidence interval generated with 10000 bootstrap replications. Specifically, IRFs are applied to the estimates of the VAR to compute responses over time in all variables to a one-unit positive shock in one of the variables. An important point is that all variables are employed in the rate of return form in the estimation of the VAR. Hence, a one-unit positive shock can be seen as a one-percentage-point positive shock. The responses should be interpreted similarly. Therefore, all IRFs are interpreted in percentage-points.[23]

4 Structural Break Tests

A structural break occurs when there is an abrupt change in a time series, a regression or even a system of equations in a point of time. It can involve a change in mean and a change in the other parameters of the process of interest which in turn reduces the reliability of the empirical analyses.

Issues related to structural breaks in regressions have been extensively studied in the econometrics literature.[24] Various methods for identifying structural breaks in a single regression model have been well documented in Bai and Perron (1998, 2003a,b, 2004) and Perron and Qu (2006). However, only a few studies such as Bai et al. (1998, 2000) and Qu and Perron (2007) have dealt with structural breaks in a system of equations. The method used in these studies relies on the assumption of common breaks[25] under which breaks in different parameters[26] occur at the same date. Bai et al. (1998) provide the details of a method that assumes a single break in a multivariate system with stationary regressors. On the other hand, Bai et al. (2000) develop a method of detecting multiple structural breaks in vector autoregressive models with stationary variables.

changes in the other variables of the system in the next periods.

[22] See, Koop et al. (1996) for the details of Generalized IRFs and its advantages over the Tradiional and Orthogonolized IRFs.

[23] Note that while interpreting IRFs, all the reported responses are positive and statistically significant unless stated otherwise.

[24] See, Perron (2006) for a comprehensive literature review.

[25] A common break refers to a break that occurs in all equations at the same date. Throughout this study, breaks are assumed to occur in all equations; and hence; the term *common* is omitted.

[26] These parameters are the regression parameters and the covariance parameters (i.e., the parameters of the covariance matrix of the errors).

Qu and Perron (2007) develop a novel approach for detecting multiple structural breaks occurring at unknown dates in linear multivariate regression models with stationary variables. The Qu and Perron (2007) methodology allows structural breaks to occur in three scenarios: (1) breaks occurring only in the regression parameters; (2) breaks occurring only in the covariance parameters; and (3) breaks occurring in both the regression and covariance parameters simultaneously. One advantage of the Qu and Perron (2007) methodology is that the dates and the number of breaks are endogenously estimated rather than being imposed ex–ante like some of the methods used in the time series literature. Moreover, it allows the distribution of regressors to differ across regimes and the error process to be autocorrelated as well as conditionally heteroskedastic.

The Qu and Perron (2007) methodology can be applied to various models since it permits incorporating arbitrary valid restrictions on the model parameters. For instance, it can be applied to any VAR with multiple structural breaks where a subset of the parameters does not change across regimes. In essence, the Qu and Perron (2007) methodology is more flexible than those found in the previous studies. The following subsections present a brief description of the Qu and Perron (2007) methodology and how it is applied in this study.

4.1 Model Setup and Estimation

In order to test for multiple structural breaks in VAR with the Qu and Perron (2007) methodology, consider the k-dimensional VAR(1) presented in Eq. 9. It can be extended to a general VAR(p) without any major difficulties.

$$\mathbf{y_t} = \mathbf{c} + A_1\mathbf{y_{t-1}} + \boldsymbol{\varepsilon_t} \tag{9}$$

Assume that the dates and the total number of breaks in parameters are unknown in the system. As a matter of notation, let m denote the total number of structural breaks, T denote the sample size, and k denote the number of equations. A subscript j indexes a regime $j = (1, \ldots, m+1)$, a subscript t indexes a temporal observation $t = (1, \ldots, T)$, and a subscript i indexes the equation $i = (1, \ldots, k)$ to which a scalar dependent variable y_{it} is associated. The break dates are denoted by the vector $\mathcal{T} = (T_1, \ldots, T_m)$, where $T_0 = 1$ and $T_{m+1} = T$. Hence, there are $m + 1$ unknown regimes with $T_{j-1} + 1 \leq t \leq T_j$ for $j = (1, \ldots, m + 1)$. The parameter q denotes the number of regressors and $\mathbf{z_t} = (z_{1t}, \ldots, z_{qt})'$ is the set of regressors from all equations.[27] Consequently, the model in Eq. 9 can be written in a concise form as

$$\mathbf{y_t} = (I_k \otimes \mathbf{z_t'})S\beta_\mathbf{j} + \boldsymbol{\varepsilon_t} \tag{10}$$

[27]For any VAR, $\mathbf{z_t}$ contains the deterministic terms and the lagged variables. For instance, it becomes $\mathbf{z_t} = (1, y_{1t-1}, \ldots, y_{kt-1})'$ for the k-dimensional VAR(1) presented in Eq. 9.

where I_k is a $k \times k$ identity matrix; $\beta_{\mathbf{j}}$ is a $p \times 1$ vector of regression parameters[28] in regime j, where p is the total number of regression parameters used in the system; and $\varepsilon_{\mathbf{t}}$ is the error terms with zero mean and covariance matrix Σ_j, which defines the covariance matrix in regime j. The matrix S is of dimension $kq \times p$ with full column rank. It is used to specify which regressors appear in each equation by involving elements that are zero or one. Hence, it is called *selection matrix*.[29] The Qu and Perron (2007) methodology also allows the imposition of a set of r parameter restrictions in the form of

$$g(\beta, vec(\Sigma)) = 0 \tag{11}$$

where $\beta = (\beta_1', \ldots, \beta_{m+1}')'$; $\Sigma = (\Sigma_1, \ldots, \Sigma_{m+1})$; and $g(\cdot)$ is an r–dimensional vector.

The ultimate aim of the Qu and Perron (2007) methodology is to estimate $\Psi = \{\widehat{m}, \widehat{\mathcal{T}}, \widehat{\beta}, \widehat{\Sigma}\}$. For now, suppose that m is known. The estimation of m will be discussed in the next subsection. For the estimation of Eq. 10, it is convenient to rewrite the model as

$$\mathbf{y_t} = \mathbf{x_t'}\beta_{\mathbf{j}} + \varepsilon_{\mathbf{t}} \tag{12}$$

where $\mathbf{x_t'} = (I_k \otimes \mathbf{z_t'})S$. To estimate Eq. 12, the Qu and Perron (2007) methodology employs restricted quasi–maximum likelihood assuming serially uncorrelated and normally distributed errors. Then, conditional on the given break dates $\mathcal{T} = (T_1, \ldots, T_m)$, the quasi–likelihood function is defined as

$$L_T(\mathcal{T}, \beta, \Sigma) = \prod_{j=1}^{m+1} \prod_{t=T_{j-1}+1}^{T_j} f\left(y_t | x_t; \beta_j, \Sigma_j\right) \tag{13}$$

where

$$f(y_t | x_t; \beta_j, \Sigma_j) = \frac{1}{(2\pi)^{k/2} |\Sigma_j|^{1/2}} \exp\left\{-\frac{1}{2}\left[y_t - x_t'\beta_j\right]' \Sigma_j^{-1}\left[y_t - x_t'\beta_j\right]\right\} \tag{14}$$

and the quasi–likelihood ratio is

$$LR_T = \frac{\prod_{j=1}^{m+1} \prod_{t=T_{j-1}+1}^{T_j} f\left(y_t | x_t; \beta_j, \Sigma_j\right)}{\prod_{j=1}^{m+1} \prod_{t=T_{j-1}^0+1}^{T_j^0} f\left(y_t | x_t; \beta_j^0, \Sigma_j^0\right)} \tag{15}$$

where $\mathcal{T}^0 = (T_1^0, \ldots, T_m^0)$, β_j^0, and Σ_j^0 indicate the true unknown parameters. Then, the aim

[28] It becomes $\beta_{\mathbf{j}} = (c_{1j}, A_{11,j}, A_{12,j}, \ldots, A_{1k,j}, \ldots, c_{kj}, A_{k1,j}, A_{k2,j}, \ldots, A_{kk,j})'$ for the k-dimensional VAR(1) presented in Eq. 9

[29] For any VAR, the matrix S becomes a $p \times p$ identity matrix I_p since VAR uses all of the regressors in each equation by construction (i.e., $kq = p$).

is to estimate the values of $(T_1, \ldots, T_m, \beta, \Sigma)$ that maximizes LR_T subject to restrictions $g(\beta, vec(\Sigma)) = 0$. Let $lr_T(\cdot)$ denote the log–likelihood ratio and $rlr_T(\cdot)$ denote the restricted log–likelihood ratio. Then, the objective function is defined as

$$rlr_T(\mathcal{T}, \beta, \Sigma) = lr_T(\mathcal{T}, \beta, \Sigma) + \lambda' g(\beta, vec(\Sigma)) \tag{16}$$

and the estimates are

$$\left(\widehat{\mathcal{T}}, \widehat{\beta}, \widehat{\Sigma}\right) = \underset{(T_1,\ldots,T_m;\beta;\Sigma)}{\operatorname{argmax}} \; rlr_T(\mathcal{T}, \beta, \Sigma) \tag{17}$$

The maximization of Eq. 17 is taken over all partitions $\mathcal{T} = (T_1, \ldots, T_m) = ([T\lambda_1], \ldots, [T\lambda_m])$ in the set

$$\Lambda_\epsilon = \left\{(\lambda_1, \ldots, \lambda_m); |\lambda_{j+1} - \lambda_j| \geq \epsilon, \, \lambda_1 \geq \epsilon, \, \lambda_m \leq 1 - \epsilon\right\} \tag{18}$$

where ϵ is an arbitrarily small positive number between zero and one; and [ ] denotes the integer part of the argument. The parameter ϵ is a trimming fraction that imposes a minimal length for each regime. Thus, it is called *trimming parameter*. An important result of the Qu and Perron (2007) methodology is that the estimates of the break dates $\mathcal{T} = (T_1, \ldots, T_m)$ are not affected by the restrictions imposed on the parameters β and Σ. Instead, the estimates of the break dates are only affected by the underlying structure of the system.

4.2 Selection of the Total Number of Breaks

In order to estimate the total number of breaks m, Qu and Perron (2007) use a likelihood ratio test of no structural breaks against m structural breaks. For the given partitions $\mathcal{T} = (T_1, \ldots, T_m) = ([T\lambda_1], \ldots, [T\lambda_m])$, the model can be estimated by quasi–maximum likelihood with the parameter restrictions. Thus, the test is the maximum value of the likelihood ratio over all admissible partitions in the set Λ_ϵ defined in Eq. 18. Then, the test can be constructed as

$$\begin{aligned} \sup LR_T(m, p_b, n_{bd}, n_{bo}, \epsilon) &= \sup_{(\lambda_1,\ldots\lambda_m)\in\Lambda_\epsilon} 2\left[\log \widehat{L}_T\left(\widehat{T}_1, \ldots, \widehat{T}_m\right) - \log \widetilde{L}_T\right] \\ &= 2\left[\log \widehat{L}_T\left(\widehat{T}_1, \ldots, \widehat{T}_m\right) - \log \widetilde{L}_T\right] \end{aligned} \tag{19}$$

where $\log \widehat{L}_T(\widehat{T}_1, \ldots, \widehat{T}_m)$ is the maximum of the log–likelihood obtained by considering only those partitions in Λ_ϵ; $\log \widetilde{L}_T$ is the maximum of the log–likelihood under the null hypothesis of no structural breaks; p_b is the total number of regression parameters that are allowed to change; and n_{bd} and n_{bo} respectively indicate the total number of diagonal and off–diagonal parameters of the covariance matrix of the errors that are allowed to change. As noted before, the Qu and Perron (2007) methodology is particularly flexible in testing many cases of structural breaks. For instance, using the $\sup LR_T(m, p_b, n_{bd}, n_{bo}, \epsilon)$ test, it is possible to test: (1) breaks only in the regression parameters (i.e., $n_{bd} = 0$ and $n_{bo} = 0$); (2) breaks only in the covariance parameters (i.e., $p_b = 0$); and (3) breaks in both the regression and covariance parameters simultaneously

(i.e., $p_b \neq 0$, $n_{bd} \neq 0$, and $n_{bo} \neq 0$), which is called *complete pure structural break*.

In empirical applications, it is often the case that the total number of breaks in the system is unknown. Therefore, it needs to be determined by a statistical procedure. In this regard, Qu and Perron (2007) consider a sequential testing procedure based on the null hypothesis of ℓ breaks versus the alternative hypothesis of $(\ell + 1)$ breaks. The procedure performs a one break test for each of the $(\ell + 1)$ segments defined by the partition $(\widehat{T}_1, \ldots, \widehat{T}_\ell)$ and assesses whether the maximum of the tests is significant. More precisely, the test is defined as

$$SEQ_T(\ell + 1 \mid \ell) = \max_{1 \leq j \leq \ell+1} \sup_{\tau \in \Lambda_{j,\epsilon}} lr_T\left(\widehat{T}_1, \ldots, \widehat{T}_{j-1}, \tau, \widehat{T}_j, \ldots, \widehat{T}_\ell\right) - lr_T\left(\widehat{T}_1, \ldots, \widehat{T}_\ell\right) \tag{20}$$

where $lr_T(\cdot)$ denotes the log–likelihood ratio; $(\widehat{T}_1, \ldots, \widehat{T}_\ell)$ denotes the optimal partition if ℓ breaks are assumed; and $\Lambda_{j,\epsilon} = \{\tau; \widehat{T}_{j-1} + (\widehat{T}_j - \widehat{T}_{j-1})\epsilon \leq \tau \leq \widehat{T}_{j-1} - (\widehat{T}_j - \widehat{T}_{j-1})\epsilon\}$.

Qu and Perron (2007) also consider a set of tests based on the null hypothesis of no breaks against the alternative hypothesis of an unknown number of breaks given some upper–bound M for m. These tests are called *double maximum tests* since they are based on the maximum of the weighted individual tests for the null hypothesis of no breaks against $m = (1, \ldots, M)$ breaks. The general form of the double maximum test is given as

$$D \max LR_T(M) = \max_{1 \leq m \leq M} \alpha_m \sup LR_T(m, p_b, n_{bd}, n_{bo}, \epsilon) \tag{21}$$

where α_m denotes the weight for $m = (1, \ldots, M)$. For equal weights (i.e., $\alpha_m = 1$), the test is denoted by $UD \max LR_T(M)$. Whereas, the test is denoted by $WD \max LR_T(M)$ if it applies weights to the individual tests such that the marginal p–values are equal across values of m. A detailed discussion of these tests can be found in Bai and Perron (1998, 2003b).

In practice, Qu and Perron (2007) suggest using the following strategy to determine the number of structural breaks. First, perform one of the double maximum tests to see if at least one break is present. If the test rejects, then the number of breaks can be decided based on testing $SEQ_T(\ell + 1 \mid \ell)$ sequentially until there is no rejection of the null hypothesis.[30] According to Bai and Perron (1998, 2003b), this method leads to the best results and is recommended for empirical applications.[31]

5 Estimation and Results

Using the entire data and assuming no structural breaks, each series is initially tested for seasonal unit root. None of the series are found to have a seasonal unit root in the Osborn–Chui–Smith–Birchenhall and Canova–Hansen tests. Thus, there is no need for seasonal

[30] In sequential testing, ignore the $SEQ_T(1 \mid 0)$ test and select m such that the $SEQ_T(\ell+1 \mid \ell)$ tests are insignificant for $m \leq \ell$).

[31] GAUSS code for the Qu and Perron (2007) methodology and some other explanatory documentation can be found in URL: `https://tinyurl.com/y54yfsrx`.

differencing in any of the series.

The EAP is first used to reveal whether each series is a TSP or a DSP. These results are omitted since none of the series with any lag lengths are found to be a TSP at the 5% significance level. Thus, all series are concluded to be either a stationary process or a DSP. Table 3 presents the ADF unit root test results with EAP for each series. Each series shows evidence for being a stationary process at the 5% significance level. The PP unit root test results for each series are presented in Table 4. The results suggest that each series is stationary since the null hypothesis can be rejected at any conventional significance levels. Table 5 presents the ERS unit root test results for each series, which are similar to the PP unit root test results. The KPSS stationary test results for each series are presented in Table 6. The results indicate that all of the series exhibit a unit root process when only a constant is added to the model. However, they seem to be stationary when there is a trend in the model. In overall, considering all of the unit root and stationary tests, it is decided that each series is a stationary process.

After each series is confirmed to be a stationary process, a 3-dimensional VAR is constructed with one lag (i.e., VAR(1)). Then, two structural breaks are endogenously estimated for the VAR(1) using the Qu and Perron (2007) methodology presented in Section 4. The Qu and Perron (2007) methodology is performed under the following conditions: (1) the maximum number of breaks is fixed to $m = 2$ in order to target the extreme events occurred in the history of cryptocurrencies; (2) all of the regression and covariance parameters are allowed to change across regimes; and (3) the trimming parameter is fixed to $\epsilon = 0.25$ to prevent possible size distortions of structural break tests (Bai and Perron, 2003b).

The Qu and Perron (2007) methodology is applied to the VAR(1) in two steps. In the first step, various tests are conducted to provide statistical evidence for two structural breaks. First, $WD\max LR_T(M)$ test is performed to test the null hypothesis of no breaks against the alternative hypothesis of up to two breaks.[32] The test result suggests that there is at least one structural break since the null hypothesis is rejected at the 1% significance level. Second, the $SEQ_T(\ell+1 \mid \ell)$ test presented in Eq. 20 is applied. It is a sequential testing procedure based on the null hypothesis of l breaks versus the alternative hypothesis of $(l+1)$ breaks. The $SEQ_T(2 \mid 1)$ test result indicates that there are two structural breaks since the null hypothesis of one break is rejected at the 1% significance level.[33] In the second step, the two structural break dates are endogenously estimated using the $\sup LR_T(m, p_b, n_{bd}, n_{bo}, \epsilon)$ test presented in Eq. 19. According to test results, the estimated structural break dates are 11-12-2015 and 09-28-2016. Both break dates are statistically significant at the 1% significance level.

As a result, 11-12-2015 (i.e., the 590$^{\text{th}}$ observation) and 09-28-2016 (i.e., the 911$^{\text{th}}$ observation) are selected as the two structural break dates for the 3–dimensional VAR(1). The first break date might be linked to two distinct events. On September 17, 2015, the U.S. Commodity Futures Trading Commission (CFTC) filed charges against a cryptocurrency exchange for allowing

[32] The $WD\max LR_T(M)$ test is one of the double maximum tests whose general form is presented in Eq. 21.
[33] In sequential testing, the $SEQ_T(1 \mid 0)$ test is ignored as suggested by Bai and Perron (1998, 2003b).

trade of option contracts.[34] Thus, the CFTC for the first time declared that cryptocurrencies are properly defined as commodities. On October 22, 2015, the European Court of Justice ruled that the exchange of cryptocurrencies is not subject to value–added–tax in the European Union.[35] Hence, the ruling classified cryptocurrencies as currency, instead of goods or property. On the other hand, it seems that the second structural break occurred just seventy–nine days after the 2nd halving of the Bitcoin blockchain. Considering the fact that miners gradually adjust their cost/revenue analysis to the new reward per block after the halving, the date 09-28-2016 is a close estimation for the 2nd halving of the Bitcoin blockchain occurred in 07-09-2016.

In summary, the results of the structural break tests suggest that the three rival cryptocurrencies (i.e., Bitcoin, Litecoin, and Ripple) as a system have experienced two critical structural breaks in the fourth quarter of 2015 and 2016. Therefore, it can be said that price dynamics of these cryptocurrencies have been significantly changed, and the 3–dimensional VAR(1) performed on the entire data might not be adequate to capture the true price dynamics. To capture the price dynamics before and after the structural breaks and to compare them, the data are separated into three segments on the break dates. While splitting the data into three segments, no transition period is considered.

5.1 Segment 1

This section presents the empirical results for the 1st segment.

Each series is tested for seasonal unit root with the two tests mentioned before, and none of the series are found to have a seasonal unit root in any of the tests. The results of the unit root and stationary tests are omitted since they are similar to the results presented for the entire data (see, Table 3 through Table 6). Therefore, it is concluded that each series in the 1st segment is stationary.

After each series is confirmed to be a stationary process, a 3-dimensional VAR is estimated with one lag. The VAR(1) results along with some model statistics are presented in Table 10. A series of multivariate and univariate diagnostic tests for the model residuals are presented in Table 11. According to the results, there appears to be a statistically significant serial correlation, conditional heteroskedasticity, and non–normality in the multivariate case. In overall, the results of the univariate case is similar. However, if one lag is used, it seems that *XRP* equation has homoskedastic residuals and there is no serial correlation in any of the equations. In general, these results indicate that the lag length specified for the VAR(1) should be increased. Therefore, the same model is estimated with various higher lag lengths. However, results of the model diagnostic tests do not improve. Therefore, rest of the analyses are conducted on the above–presented model.

Granger–causality tests are performed to reveal causalities between the variables of VAR(1). The results in Table 12 show that there is a unidirectional Granger–causality between *BTC-XRP*.

[34] See URL: `https://tinyurl.com/yxjsval3`.
[35] See URL: `https://goo.gl/frSf8y`.

In essence, these are the only variables that exhibit a Granger–causality in the system.

Finally, impulse response analysis is performed for the 1st segment. Figure 3 illustrates the responses of all variables to a one-percentage-point positive shock in each variable individually. What stands out in these results is that all impulses yield an immediate positive impact, and they die out rapidly and reach zero (i.e., the effect of an impulse is transitory) as expected due to the stable system. The results suggest that a one-percentage-point positive shock in *BTC* yields a statistically significant but gradually decreasing impact on itself, and it dies out after four days. The same impulse causes an immediate 1.05 percentage-point increase in *LTC*, which gradually decreases toward zero and becomes statistically insignificant after two days. The same shock leads to an immediate 0.35 percentage-point increase in *XRP*; however, it dies out rapidly and becomes statistically insignificant before the end of the first day. A one-percentage-point positive shock in *LTC* generates a statistically significant but gradually decreasing effect in itself until the fourth day. The same shock leads to an immediate 0.35 percentage-point increase in *BTC*, which stays statistically significant until the fourth day and then dies out. The same impulse generates an immediate 0.2 percentage-point increase in *XRP* but rapidly dies out and becomes insignificant just after the first day. A similar shock in *XRP* leads to immediate 0.12 and 0.22 percentage-point increases in *BTC* and *LTC* respectively; however, these impacts die out and become statistically insignificant just after the first day. The response of *XRP* to own impulse gradually decreases and lasts six days before becoming statistically insignificant.

5.2 Segment 2

This section presents the empirical results for the 2nd segment.

All of the series are tested for seasonal unit root, and it is found that none of the series exhibits a seasonal unit root process in any of the two tests mentioned before. Then, the unit root and stationary tests are applied to each series, but the results are omitted since they are similar to the results presented for the entire data (see, Table 3 through Table 6). Hence, it is decided that all of the series in the 2nd segment exhibit a stationary process.

A 3-dimensional VAR is estimated with one lag since all of the series are stationary. Table 13 provides the VAR(1) results along with some model statistics. The multivariate and univariate diagnostic tests for the model residuals are given in Table 14. The results suggest a statistically significant serial correlation, conditional heteroskedasticity, and non–normality in the multivariate case. In the univariate case, the serial correlation problem is disappeared; however, the other problems still persist. In general, it seems that the problems with the model residuals are mitigated a little bit compared to the 1st segment.

To investigate causalities between the variables, Granger–causality tests are performed. However, the results presented in Table 15 suggest no Granger–causality in the system.

Finally, impulse response analysis is performed for the 2nd segment. Figure 4 displays the responses of all variables to a one-percentage-point positive shock in each variable individually.

In overall, the results show that the responses die out quickly and reach zero as in the 1st segment. The results indicate that a one-percentage-point positive shock in *BTC* causes a statistically significant but gradually decreasing response in itself; however, it dies out after four days. The same shock leads to an immediate 0.9 percentage-point increase in *LTC*, but it gradually decreases to zero and becomes statistically insignificant after two days. The response of *XRP* to the same impulse in *BTC* is statistically insignificant throughout the days considered. A one-percentage-point positive shock in *LTC* leads to a statistically significant but gradually decreasing impact on itself until the fourth day. The same shock immediately increases *BTC* by 0.75 percentage-point, which stays statistically significant until the fourth day and dies out. The response of *XRP* to the same shock is statistically insignificant for the days considered. A similar shock in *XRP* generates statistically significant responses only in itself, which dies out in just one day.

5.3 Segment 3

This section presents the empirical results for the 3rd segment.

Each series is tested for seasonal unit root, and none of the series are found to have a seasonal unit root. Once again, the results of the unit root and stationary tests are omitted due to the similarity to the results presented for the entire data (see, Table 3 through Table 6). Thus, it is concluded that each series in the 3rd segment exhibits a stationary process.

After all of the series are confirmed to exhibit a stationary process, a 3-dimensional VAR is estimated with one lag. Table 13 presents the VAR(1) results along with some model statistics. Table 17 shows the multivariate and univariate diagnostic tests for the model residuals. It appears that the problems with the model residuals still continue as in the first two segments. The results of the multivariate case suggest that the model residuals are serially correlated, conditionally heteroskedastic, and non–normal. However, for the univariate case, the residuals are serially uncorrelated and homoskedastic in *LTC* equation only.

The Granger–causality test results are presented Table 15. The results indicate that there are unidirectional Granger–causalities between *BTC-XRP* and *LT-XRP* only.

Finally, impulse response analysis is performed for the 3rd segment. Figure 5 presents the responses of all variables to a one-percentage-point positive shock in each variable individually. Once again, the results show that the responses only last for couple days and reach zero as in the first two segments. A one-percentage-point positive shock in *BTC* generates a statistically significant but gradually decreasing response in itself, which lasts for four days then reaches zero. The same impulse immediately increases *LTC* by 0.81 percentage-point; however, it rapidly decreases and become statistically insignificant just after one day. The response of *XRP* to the same impulse leads to an immediate 0.38 percentage-point increase, but it almost instantly becomes insignificant at the beginning of the first day. A one-percentage-point positive shock in *LTC* results in a statistically significant but gradually decreasing effect in itself for three

days. The same shock immediately increases *BTC* and *XRP* by 0.25 and 0.41 percentage-point respectively, but they die out after three days and become insignificant. A similar shock in *XRP* leads to immediate 0.05 and 0.15 percentage-point increases in *BTC* and *LTC* respectively, but the impacts die out and become statistically insignificant after couple days. The response of *XRP* to own impulse gradually decreases and lasts three days before becoming statistically insignificant.

6 Discussion

A comparison of each segment provides useful insights, especially in understanding how the price dynamics between the rival cryptocurrencies change over time and are affected by structural shocks. The comparison is performed in two steps using the results of Granger–causality test and impulse response analysis.

In the first step, the Granger–causality test results presented in Table 12, Table 15, and Table 18 are compared to investigate the changes in causalities between rival cryptocurrencies across segments. The comparison shows that there is a unidirectional Granger–causality between *BTC-XRP* in the 1st and 3rd segments; however, it disappears in the 2nd segment. Moreover, a unidirectional Granger–causality between *LTC-XRP* appears only in the 3rd segment. In essence, considering the following factor might explain why *BTC* and *LTC* Granger–causes *XRP* in the 3rd segment. Bitcoin and Litecoin are often considered as the gold and silver of the cryptocurrency world due to their reliable and long history. Therefore, a price movement in these coins is interpreted as a general price change in the whole cryptocurrency market by investors. As a result, the Granger–causality test results imply that the structure of the price dynamics between the rival cryptocurrencies has changed after the structural breaks.

In order to thoroughly understand how the price dynamics have changed across segments, the impulse responses of each segment are compared impulse by impulse.

First, comparing Figure 3a, Figure 4a, and Figure 5a suggests that the response of *XRP* to a shock in *BTC* is not statistically significant only in the 2nd segment. An interesting result is that the responses of *BTC* and *LTC* to a shock in *BTC* are overall the same across segments. These results, in essence, confirm the Granger–causality tests. As a result, it is concluded that in response to a shock in Bitcoin price, the change in each coin is overall the same across segments.

Second, comparing Figure 3b, Figure 4b, and Figure 5b indicates that a one-percentage-point positive shock in *LTC* yields a 0.75 percentage-point increase in *BTC* in the 2nd segment, which is three times higher than the 3rd segment. Moreover, the same shock increases *XRP* by 0.2 and 0.41 percentage-point in the 1st and 3rd segments respectively. However, the response is not statistically significant in the 2nd segment. In overall, these results suggest that in response to a shock in Litecoin price, the impact on Bitcoin price is decreasing over time; however, the impact on Ripple price is increasing.

Third, when Figure 3c, Figure 4c, and Figure 5c are compared, it can be seen that the response

of each variable to a shock in *XRP* are statistically insignificant in the 2nd segment. Moreover, the response of *BTC* and *LTC* to the same shock are decreasing from the 1st segment to the 2nd segment. As a result, it can be said that, in overall, in response to a shock in Ripple price, the impact on the prices of Bitcoin and Litecoin are decreasing over time.

7 Conclusion

The present research provides empirical evidence on the structural change of the price dynamics between three rival cryptocurrencies (i.e., Bitcoin, Litecoin, and Ripple) over the period of April 2014-July 2017. For this purpose, first, the Qu and Perron (2007) methodology is performed to determine two structural breaks in a VAR framework. The choice of this methodology is led by its decisive advantages compared to the alternative techniques used in the literature. Specifically, the methodology endogenously estimates multiple structural breaks in regression and covariance parameters at an unknown date. It also allows the distribution of regressors to differ across regimes and the error process to be autocorrelated as well as conditionally heteroskedastic. Second, the estimated breakpoints are used to split the data into three segments. Finally, to investigate the dynamic price linkages across segments, Granger–causality tests and impulse response analysis are applied to each segment.

In overall, five conclusions can be drawn from the results. First, using the daily price data for cryptocurrencies, this study finds that there are two robust structural breaks (i.e., 11-12-2015 and 09-28-2016) that appear to have affected the price dynamics between the rival cryptocurrencies. The first break date is linked to two distinct events that declared a cryptocurrency not only as a commodity but also as currency. The second break is linked to the 2nd halving of the Bitcoin blockchain. Second, after the second structural break, the Granger–causality from the prices of other coins to Ripple price have gained strength. Third, the response of each coin to a shock in Bitcoin price is same across segments. Fourth, in response to a shock in Litecoin price, the impact on Bitcoin price is decreasing over time; however, the impact on Ripple price is increasing. Fifth, the impact on the prices of Bitcoin and Litecoin are decreasing over time in response to a shock in Ripple price.

Table 1: Data Description Summary

Variable	Description	Source	# of Obs.
Bitcoin Price	Bitcoin Price from BraveNewCoin (2017), nominal daily observations of the volume weighted average price in USD. The designated symbol for the rate of return form is BTC unless otherwise noted.	Quandl (2017)	1215
Litecoin Price	Litecoin Price from BraveNewCoin (2017), nominal daily observations of the volume weighted average price in USD. The designated symbol for the rate of return form is LTC unless otherwise noted.	Quandl (2017)	1215
Ripple Price	Ripple Price from BraveNewCoin (2017), nominal daily observations of the volume weighted average price in USD. The designated symbol for the rate of return form is XRP unless otherwise noted.	Quandl (2017)	1215

Notes: Downloaded on July 30, 2017 from Quandl (2017). The Designated symbols refer to a coin itself in the text and the transformed variable in the analyses.

Table 2: Summary Statistics - Entire Data

Variable	# of Obs.	Min.	Max.	Median	Mean	Std. Dev.	Skewness	Kurtosis
Bitcoin Price	1215	192.66	2924.81	449.81	642.50	558.17	2.47	5.85
Rate of Return Bitcoin Price	1214	−18.56	17.23	0.15	0.19	2.92	−0.32	5.75
Litecoin Price	1215	1.27	53.09	3.83	6.71	8.92	3.32	10.86
Rate of Return Litecoin Price	1214	−35.14	46.68	−0.01	0.20	4.80	1.47	17.23
Ripple Price	1215	0.00	0.38	0.01	0.03	0.06	3.65	12.27
Rate of Return Ripple Price	1214	−37.54	101.56	−0.19	0.44	6.66	4.45	55.75

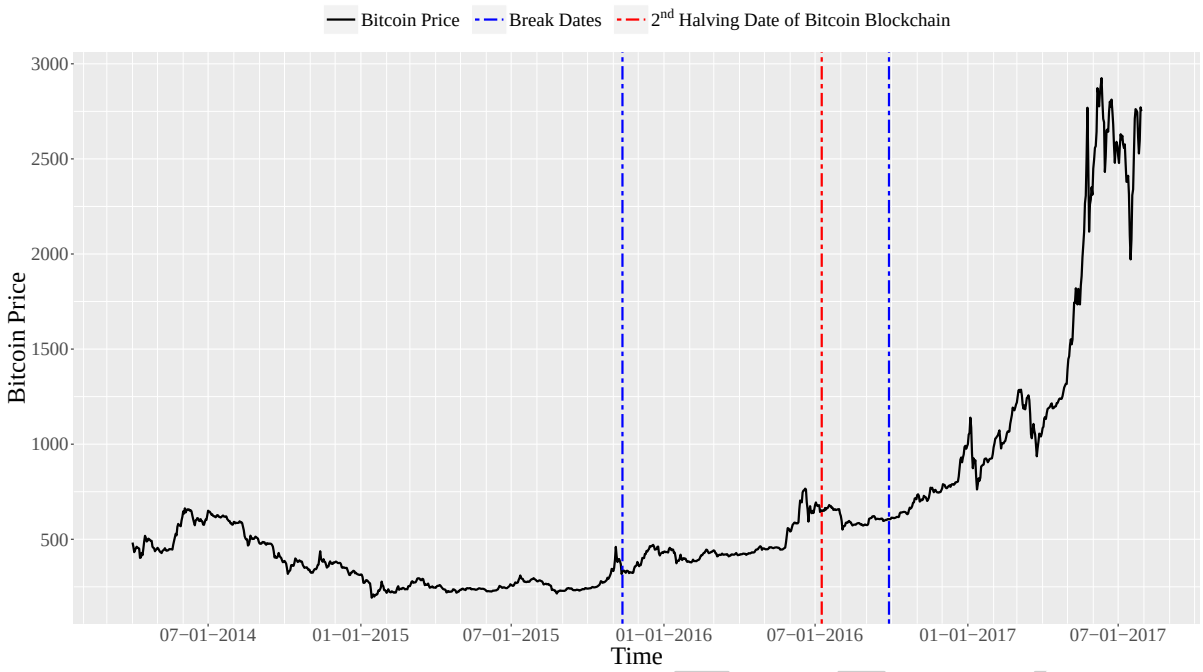

(a) Bitcoin Price

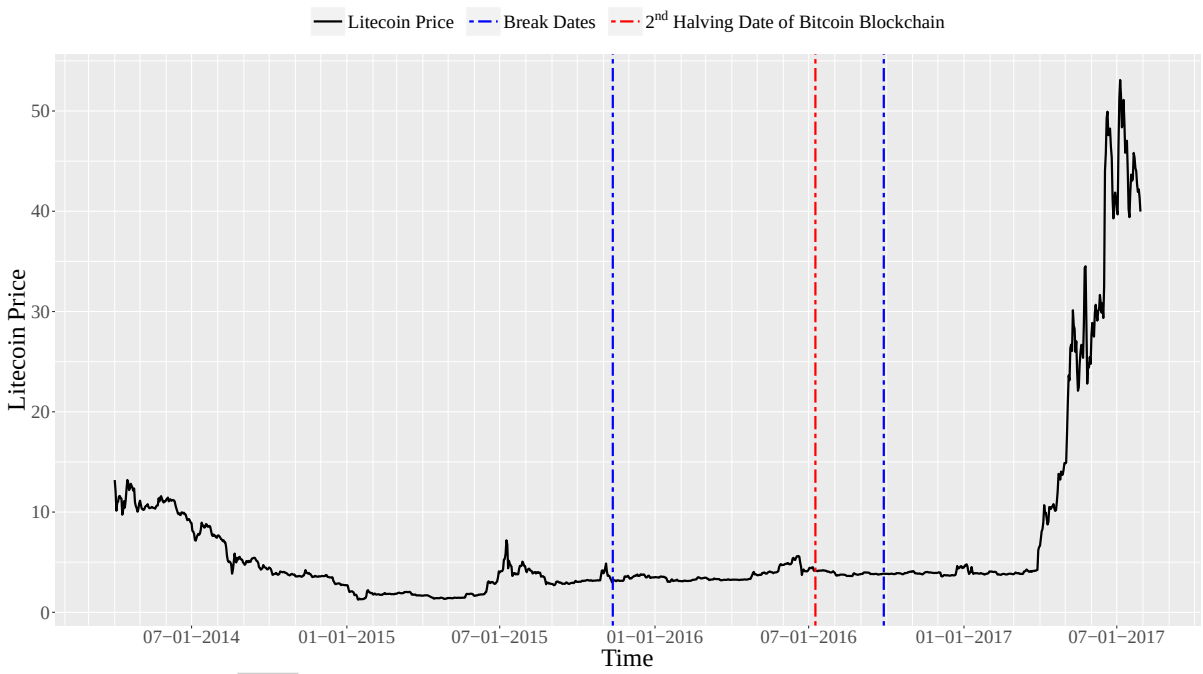

(b) Litecoin Price

Figure 1: Plots of All Variables

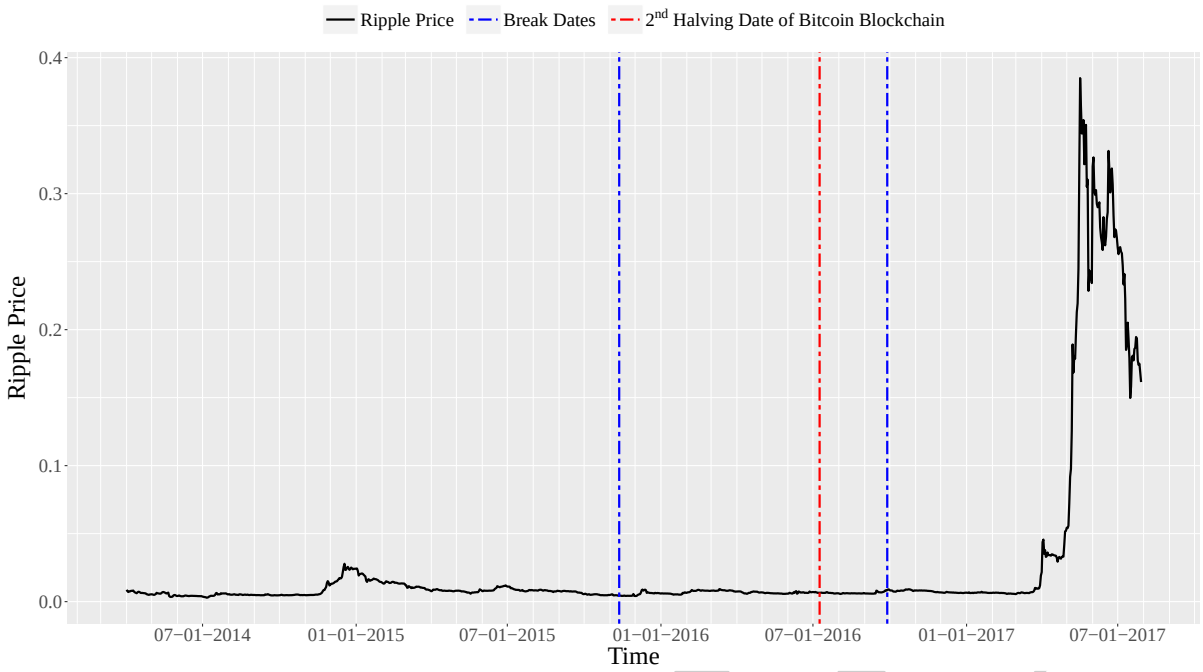

(c) Ripple Price

Figure 1 (continued)

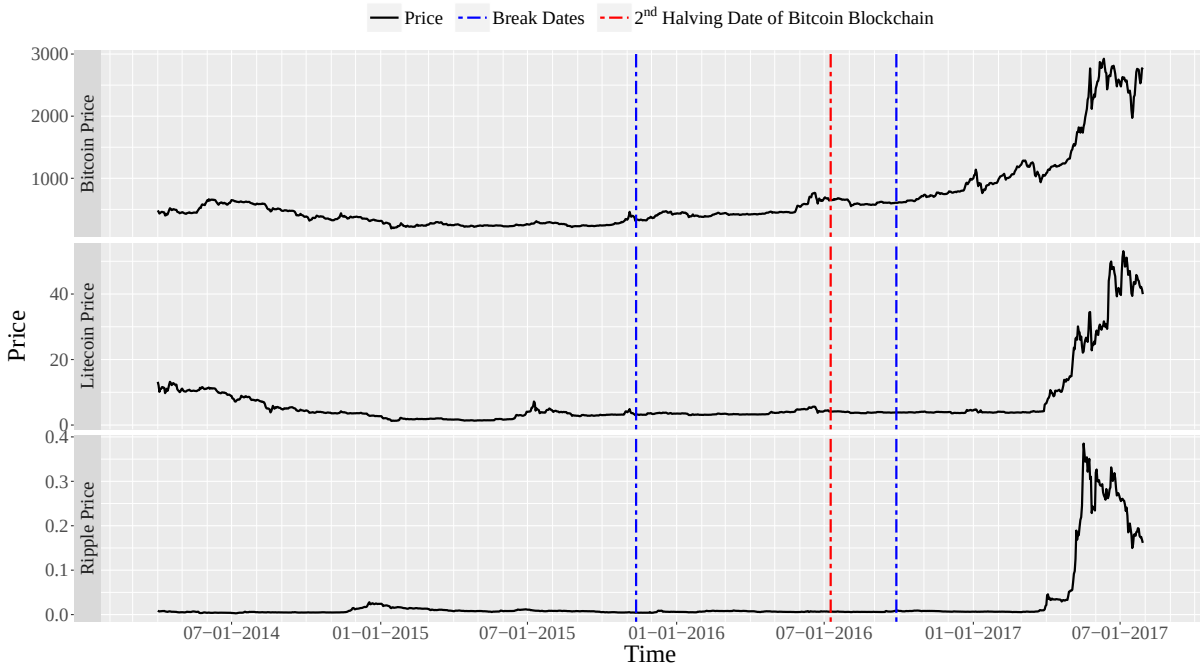

Figure 2: Plot of All Variables Together

Table 3: ADF Unit Root Test Results with EAP - Entire Data

	Variable:		
Lag	BTC	LTC	XRP
AIC	Stationary	Stationary	Stationary
BIC	Stationary	Stationary	Stationary
NPS	Stationary	Stationary	Stationary

Notes: All decisions are given at the 5% significance level.

Table 4: PP Unit Root Test Statistics - Entire Data

		Variable:		
Model	Lag	BTC	LTC	XRP
Constant	AIC	-27.39^{***}	-27.92^{***}	-28.38^{***}
	BIC	-27.68^{***}	-28.12^{***}	-27.85^{***}
	Long	-27.16^{***}	-28.06^{***}	-29.69^{***}
	Short	-27.23^{***}	-27.92^{***}	-28.28^{***}
Trend	AIC	-27.52^{***}	-28.05^{***}	-28.42^{***}
	BIC	-27.80^{***}	-28.32^{***}	-27.94^{***}
	Long	-27.14^{***}	-27.94^{***}	-29.56^{***}
	Short	-27.32^{***}	-28.05^{***}	-28.33^{***}

Notes: *, **, and *** indicate statistical significance at the 10%, 5%, and 1% levels respectively.

Table 5: ERS Unit Root Test Statistics - Entire Data

		Variable:		
Model	Lag	BTC	LTC	XRP
Constant	AIC	-6.27^{***}	-2.79^{***}	-2.17^{**}
	BIC	-9.27^{***}	-8.60^{***}	-8.02^{***}
	Long	-0.94	-0.94	-1.28
	Short	-2.81^{***}	-2.79^{***}	-2.61^{***}
Trend	AIC	-11.54^{***}	-5.62^{***}	-4.22^{***}
	BIC	-16.35^{***}	-15.48^{***}	-13.89^{***}
	Long	-2.65^{*}	-2.32	-2.74^{*}
	Short	-5.71^{***}	-5.62^{***}	-5.02^{***}

Notes: *, **, and *** indicate statistical significance at the 10%, 5%, and 1% levels respectively.

Table 6: KPSS Stationary Test Statistics - Entire Data

		Variable:		
Model	Lag	BTC	LTC	XRP
Constant	AIC	0.70**	0.87***	0.45*
	BIC	0.71**	0.99***	0.64**
	Long	0.66**	0.77***	0.33
	Short	0.67**	0.87***	0.45*
Trend	AIC	0.03	0.08	0.13*
	BIC	0.04	0.09	0.19**
	Long	0.04	0.08	0.10
	Short	0.03	0.08	0.13*

Notes: *, **, and *** indicate statistical significance at the 10%, 5%, and 1% levels respectively.

Table 7: Summary Statistics - Segment 1

Variable	# of Obs.	Min.	Max.	Median	Mean	Std. Dev.	Skewness	Kurtosis
Rate of Return Bitcoin Price	589	−18.56	17.23	−0.08	−0.03	3.02	−0.20	6.70
Rate of Return Litecoin Price	589	−35.14	32.11	−0.14	−0.12	5.09	0.42	10.55
Rate of Return Ripple Price	589	−37.54	28.27	−0.21	0.01	5.03	0.17	9.73

Table 8: Summary Statistics - Segment 2

Variable	# of Obs.	Min.	Max.	Median	Mean	Std. Dev.	Skewness	Kurtosis
Rate of Return Bitcoin Price	321	−9.63	11.40	0.16	0.23	2.31	0.19	5.74
Rate of Return Litecoin Price	321	−18.20	11.90	0.02	0.11	2.50	−0.77	12.91
Rate of Return Ripple Price	321	−25.02	34.90	−0.05	0.33	5.27	1.34	13.38

Table 9: Summary Statistics - Segment 3

Variable	# of Obs.	Min.	Max.	Median	Mean	Std. Dev.	Skewness	Kurtosis
Rate of Return Bitcoin Price	304	−14.65	11.22	0.47	0.55	3.25	−0.71	3.51
Rate of Return Litecoin Price	304	−20.67	46.68	0.18	0.93	5.89	2.59	16.26
Rate of Return Ripple Price	304	−26.35	101.56	−0.33	1.37	9.88	4.96	40.30

Table 10: VAR Results - Segment 1

	Equation:		
	BTC	LTC	XRP
Constant	−0.012	−0.084	0.022
BTC_{t-1}	0.176***	−0.018	−0.206**
LTC_{t-1}	0.046	0.211***	0.012
XRP_{t-1}	−0.003	0.009	0.317***
Observations	588	588	588
Residual Std. Error	2.946	4.991	4.764
R^2	0.052	0.043	0.102
Adjusted R^2	0.048	0.038	0.098
F Statistic	10.773***	8.672***	22.163***

Notes: All the roots are inside the unit circle, and the system is dynamically stable. *, **, and *** indicate statistical significance at the 10%, 5%, and 1% levels respectively.

Table 11: Diagnostic Test Statistics for VAR - Segment 1

		Univariate Tests by Equation:		
Test	Multivariate	BTC	LTC	XRP
$LB_{(1)}$	2.47^{***}	0.32	0.37	1.24
$LB_{(2)}$	41.51^{***}	9.93^{***}	17.50^{***}	10.73^{***}
$LB_{(3)}$	54.56^{***}	10.03^{**}	20.79^{***}	15.77^{***}
$LB_{(4)}$	57.99^{***}	10.05^{**}	20.84^{***}	15.78^{***}
$LB_{(5)}$	65.71^{***}	10.19^{*}	21.28^{***}	15.84^{***}
$LB_{(7)}$	89.01^{***}	12.18^{*}	28.26^{***}	23.78^{***}
$LB_{(10)}$	125.59^{***}	22.38^{**}	36.85^{***}	25.01^{***}
$ARCH_{(1)}$	291.77^{***}	129.53^{***}	75.66^{***}	1.53
$ARCH_{(2)}$	390.84^{***}	129.22^{***}	79.19^{***}	9.01^{**}
$ARCH_{(3)}$	453.26^{***}	129.23^{***}	81.79^{***}	10.66^{**}
$ARCH_{(4)}$	500.36^{***}	131.87^{***}	81.68^{***}	10.82^{**}
$ARCH_{(5)}$	594.07^{***}	131.64^{***}	99.77^{***}	28.58^{***}
$ARCH_{(7)}$	683.55^{***}	144.55^{***}	100.04^{***}	29.99^{***}
$ARCH_{(10)}$	820.09^{***}	158.89^{***}	102.84^{***}	31.33^{***}
JB	16155.35^{***}	768.02^{***}	2264.96^{***}	2750.99^{***}
Skewness	23.54^{***}	-0.38^{***}	0.35^{***}	-0.33^{***}
Kurtosis	16131.81^{***}	8.55^{***}	12.59^{***}	13.58^{***}

Notes: LB, ARCH, JB, Skewness, and Kurtosis indicate Ljung–Box test for autocorrelation, ARCH test for autoregressive conditional heteroskedasticity, Jarque–Bera test for normality, Skewness test for only skewness, and Kurtosis test for only kurtosis respectively. Values in parenthesis indicate the lag length used in LB and ARCH tests. *, **, and *** indicate statistical significance at the 10%, 5%, and 1% levels respectively.

Table 12: Granger–Causality Test Statistics - Segment 1

	BTC	LTC	XRP
BTC		0.04	5.79^{**}
LTC	2.23		0.06
XRP	0.01	0.04	

Notes: Value in each cell indicates the test statistics for the hypothesis H_0 that is the row variable does not Granger–cause the column variable. *, **, and *** indicate statistical significance at the 10%, 5%, and 1% levels respectively.

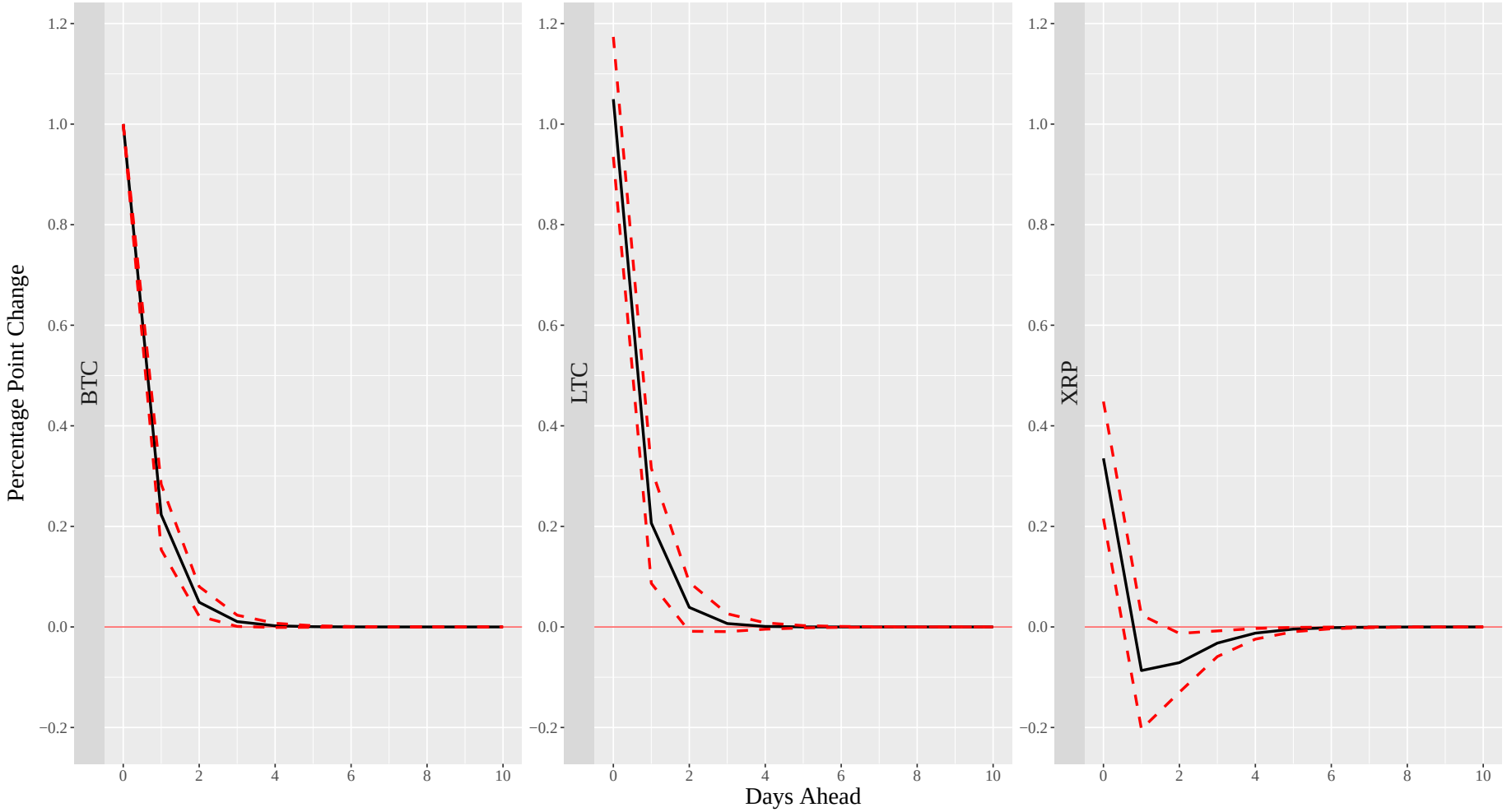

Notes: All variables are in the rate of return form in the estimation, but the interpretation of IRFs is in percentage point change with a 90% confidence interval generated with 10000 bootstrap replications.

(a) Response of All Variables to a One-Percentage-Point Positive Shock in Rate of Return Bitcoin Price - Segment 1

Figure 3: Impulse Responses Analysis - Segment 1

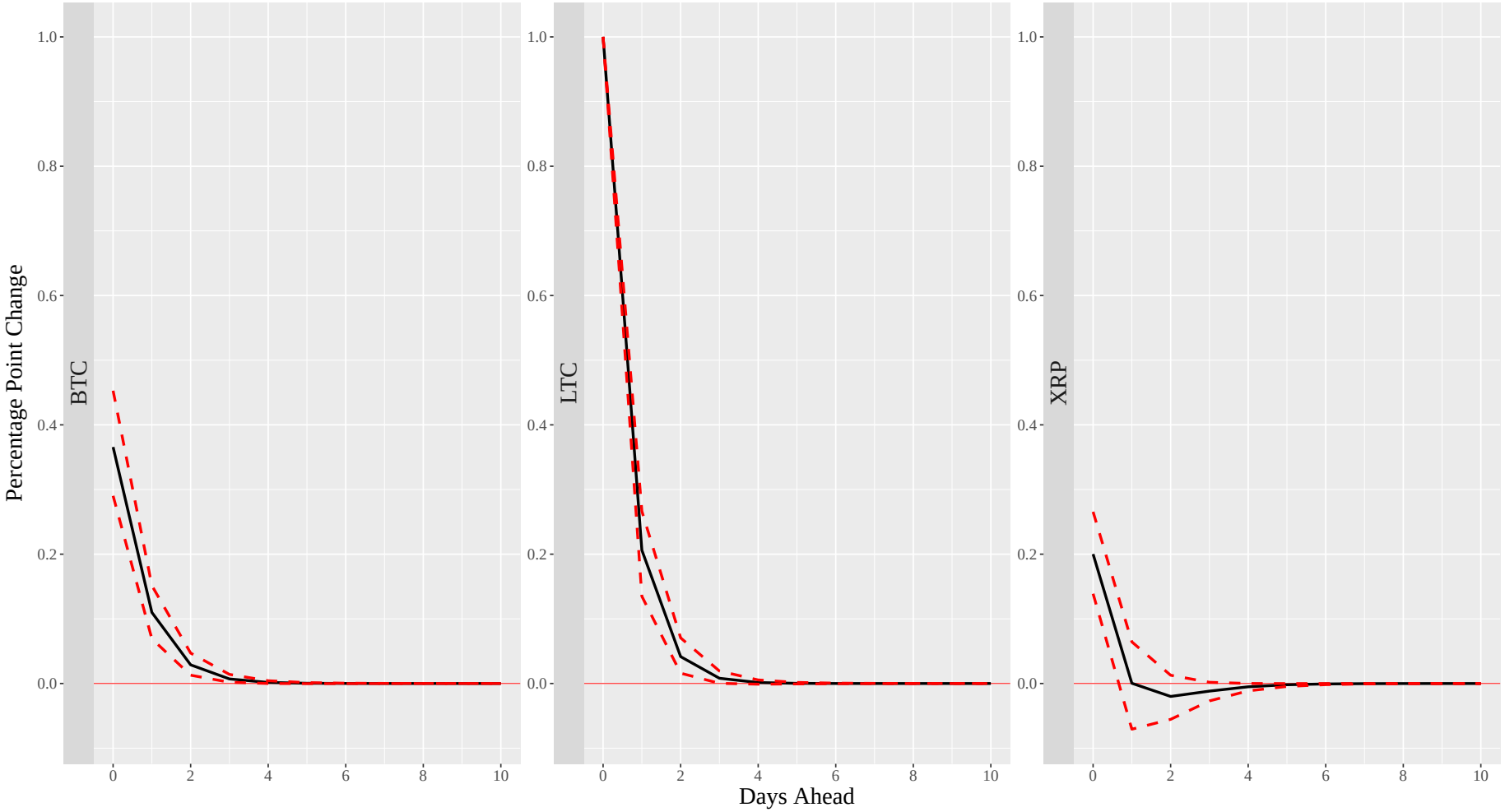

Notes: All variables are in the rate of return form in the estimation, but the interpretation of IRFs is in percentage point change with a 90% confidence interval generated with 10000 bootstrap replications.

(b) Response of All Variables to a One-Percentage-Point Positive Shock in Rate of Return Litecoin Price - Segment 1

Figure 3 (continued)

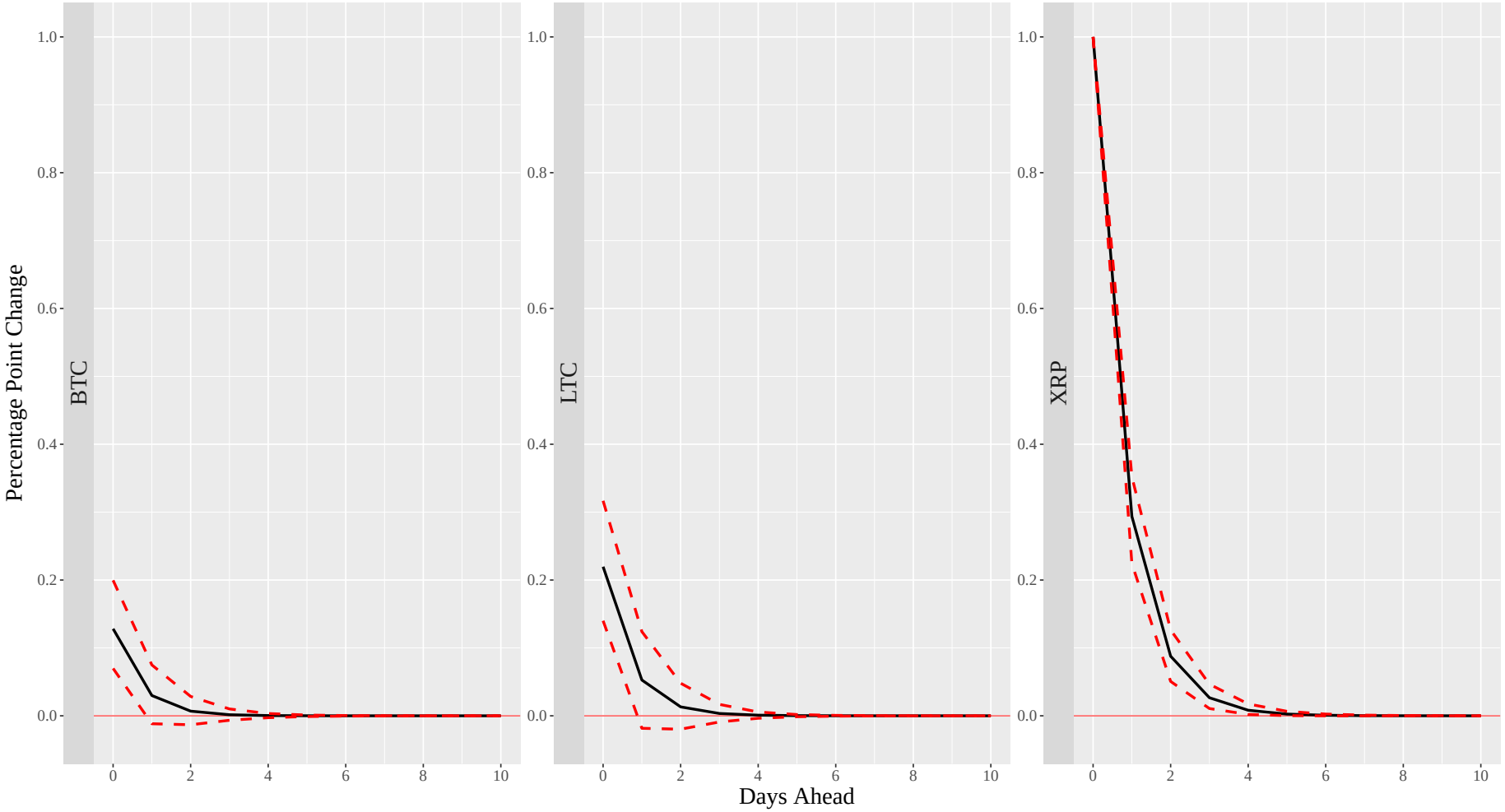

Notes: All variables are in the rate of return form in the estimation, but the interpretation of IRFs is in percentage point change with a 90% confidence interval generated with 10000 bootstrap replications.

(c) Response of All Variables to a One-Percentage-Point Positive Shock in Rate of Return Ripple Price - Segment 1

Figure 3 (continued)

Table 13: VAR Results - Segment 2

	Equation:		
	BTC	LTC	XRP
Constant	0.161	0.071	0.260
BTC_{t-1}	0.160	−0.084	0.370
LTC_{t-1}	0.052	0.248**	−0.300
XRP_{t-1}	0.039	0.042	0.027
Observations	320	320	320
Residual Std. Error	2.255	2.445	5.274
R^2	0.052	0.043	0.009
Adjusted R^2	0.043	0.034	0.000
F Statistic	5.817***	4.713***	0.999

Notes: All the roots are inside the unit circle, and the system is dynamically stable. *, **, and *** indicate statistical significance at the 10%, 5%, and 1% levels respectively.

Table 14: Diagnostic Test Statistics for VAR - Segment 2

		Univariate Tests by Equation:		
Test	Multivariate	BTC	LTC	XRP
$LB_{(1)}$	0.46^{***}	0.10	0.03	0.01
$LB_{(2)}$	27.05^{***}	5.85^{*}	1.79	8.65^{**}
$LB_{(3)}$	41.55^{***}	6.47^{*}	3.04	9.89^{**}
$LB_{(4)}$	58.17^{***}	6.62	3.18	11.00^{**}
$LB_{(5)}$	64.32^{***}	9.26^{*}	4.91	11.02^{*}
$LB_{(6)}$	75.57^{***}	11.96^{*}	4.96	11.76^{*}
$LB_{(7)}$	84.12^{***}	12.01	5.09	11.97
$LB_{(10)}$	106.62^{**}	13.10	7.41	12.91
$ARCH_{(1)}$	188.34^{***}	22.48^{***}	58.09^{***}	9.85^{***}
$ARCH_{(2)}$	272.11^{***}	25.89^{***}	58.15^{***}	10.91^{***}
$ARCH_{(3)}$	316.87^{***}	30.37^{***}	58.40^{***}	11.15^{**}
$ARCH_{(4)}$	369.52^{***}	30.37^{***}	61.45^{***}	12.26^{**}
$ARCH_{(5)}$	409.11^{***}	30.81^{***}	61.56^{***}	12.20^{**}
$ARCH_{(6)}$	469.18^{***}	31.06^{***}	61.40^{***}	13.88^{**}
$ARCH_{(7)}$	492.67^{***}	31.57^{***}	61.54^{***}	13.89^{*}
$ARCH_{(10)}$	675.44^{***}	37.09^{***}	62.15^{***}	21.94^{**}
JB	4228.79^{***}	660.94^{***}	2723.82^{***}	2557.50^{***}
Skewness	98.68^{***}	0.52^{***}	−0.15	1.27^{***}
Kurtosis	4130.10^{***}	9.96^{***}	17.29^{***}	16.61^{***}

Notes: LB, ARCH, JB, Skewness, and Kurtosis indicate Ljung–Box test for autocorrelation, ARCH test for autoregressive conditional heteroskedasticity, Jarque–Bera test for normality, Skewness test for only skewness, and Kurtosis test for only kurtosis respectively. Values in parenthesis indicate the lag length used in LB and ARCH tests. *, **, and *** indicate statistical significance at the 10%, 5%, and 1% levels respectively.

Table 15: Granger–Causality Test Statistics - Segment 2

	BTC	LTC	XRP
BTC		0.63	2.65
LTC	0.34		2.05
XRP	2.69	2.57	

Notes: Value in each cell indicates the test statistics for the hypothesis H_0 that is the row variable does not Granger–cause the column variable. *, **, and *** indicate statistical significance at the 10%, 5%, and 1% levels respectively.

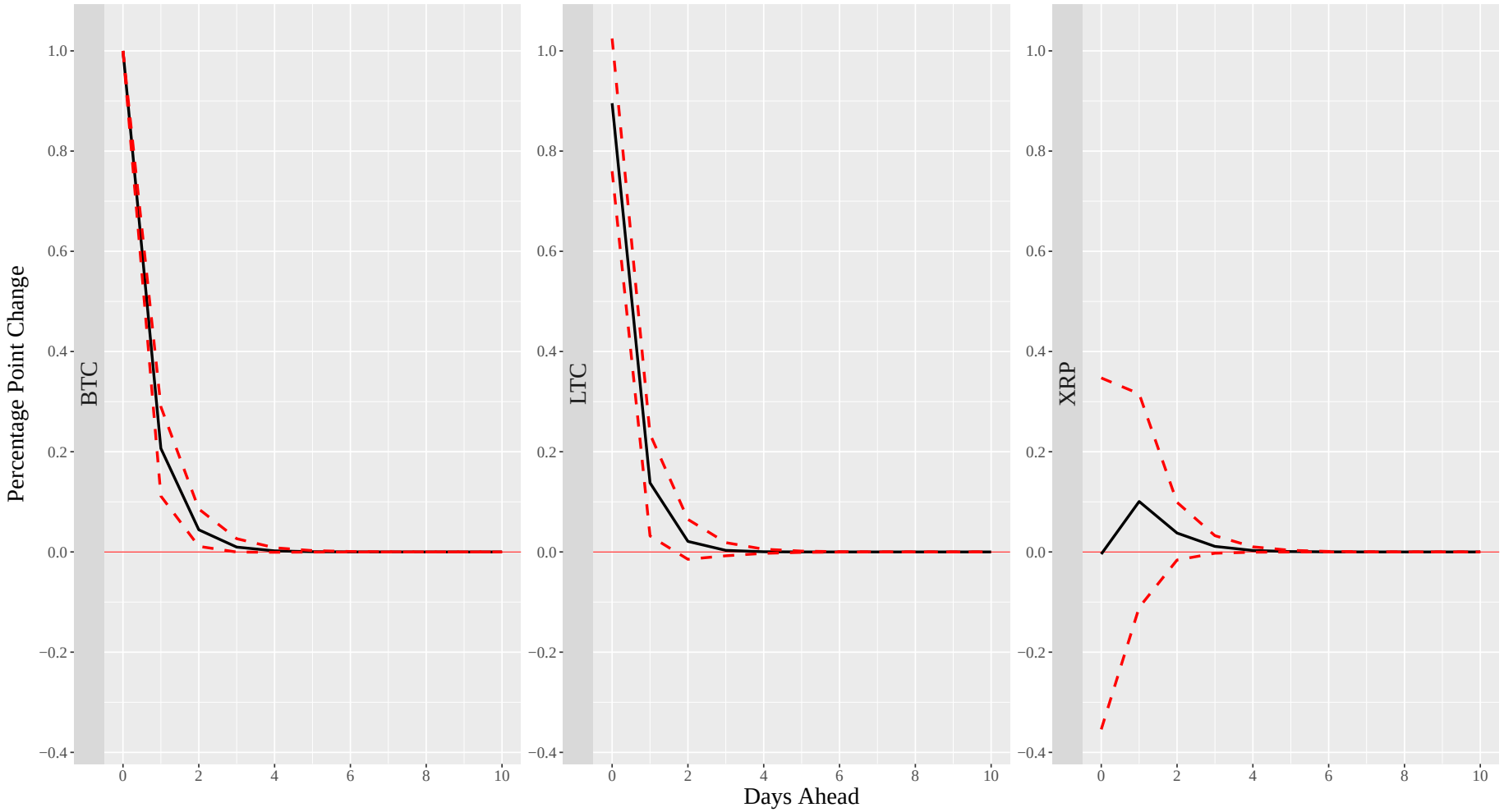

Notes: All variables are in the rate of return form in the estimation, but the interpretation of IRFs is in percentage point change with a 90% confidence interval generated with 10000 bootstrap replications.

(a) Response of All Variables to a One-Percentage-Point Positive Shock in Rate of Return Bitcoin Price - Segment 2

Figure 4: Impulse Responses Analysis - Segment 2

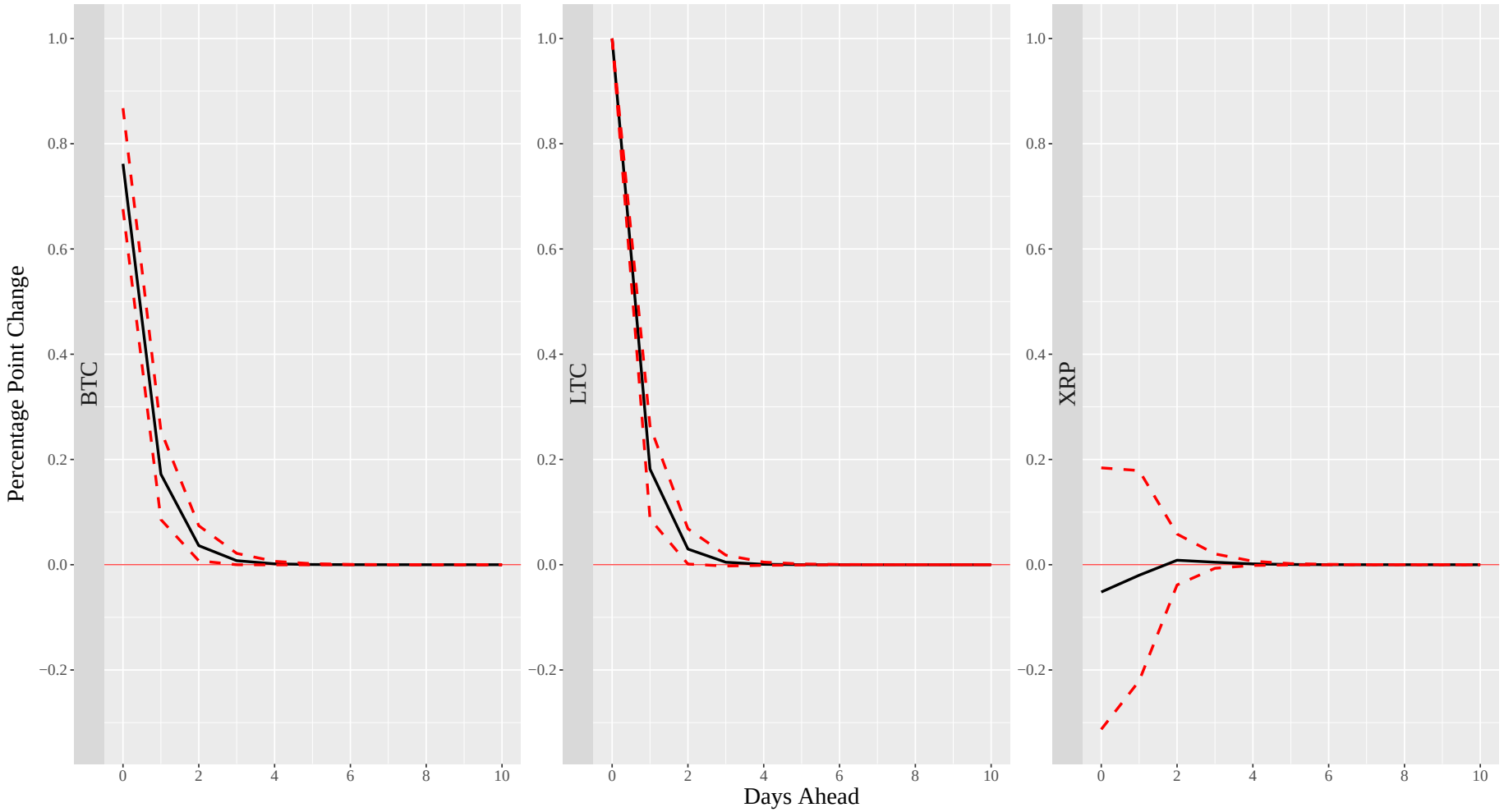

Notes: All variables are in the rate of return form in the estimation, but the interpretation of IRFs is in percentage point change with a 90% confidence interval generated with 10000 bootstrap replications.

(b) Response of All Variables to a One-Percentage-Point Positive Shock in Rate of Return Litecoin Price - Segment 2

Figure 4 (continued)

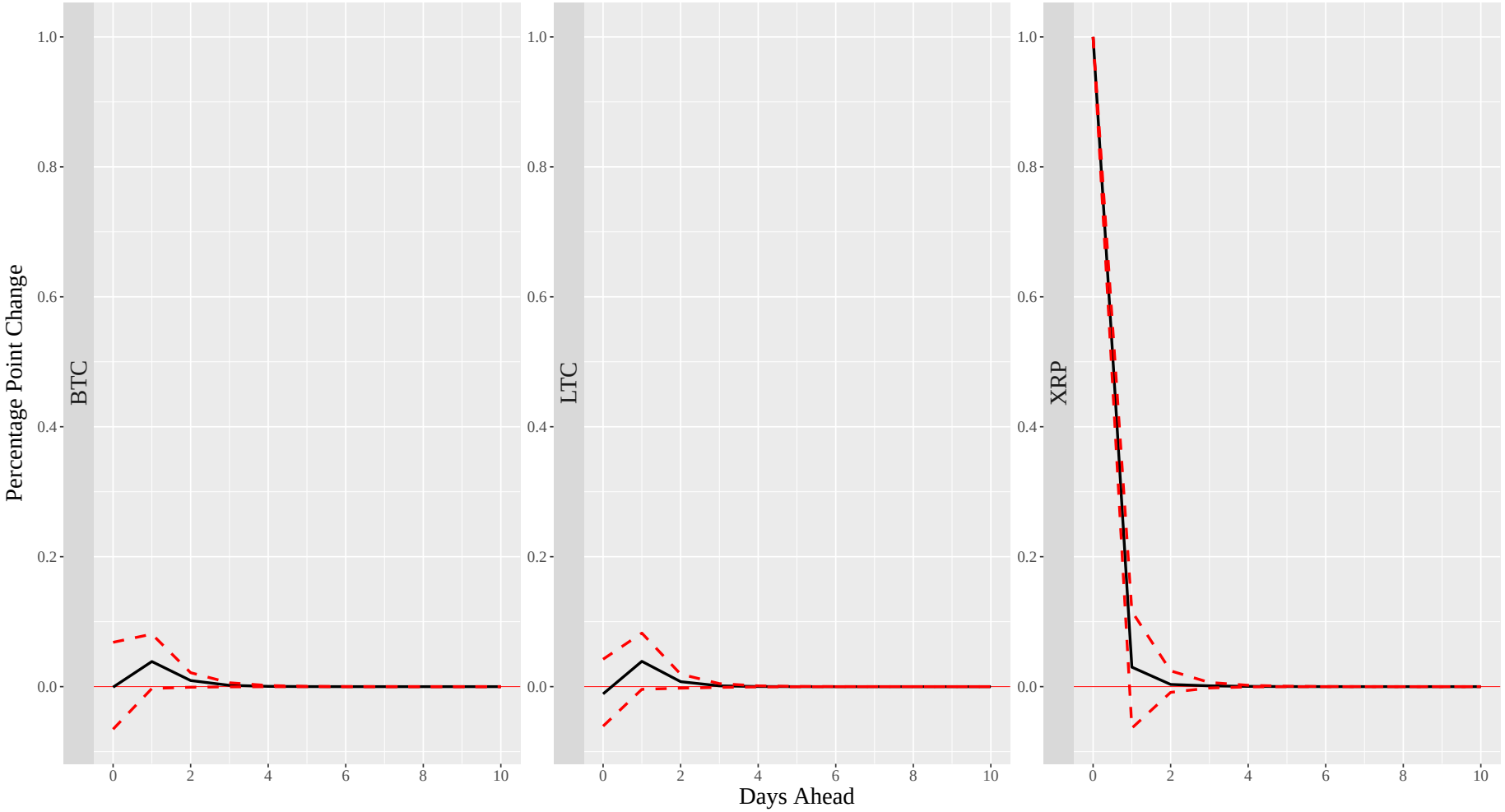

Notes: All variables are in the rate of return form in the estimation, but the interpretation of IRFs is in percentage point change with a 90% confidence interval generated with 10000 bootstrap replications.

(c) Response of All Variables to a One-Percentage-Point Positive Shock in Rate of Return Ripple Price - Segment 2

Figure 4 (continued)

Table 16: VAR Results - Segment 3

	Equation:		
	BTC	LTC	XRP
Constant	0.364**	0.727**	0.915
BTC_{t-1}	0.223***	−0.035	−0.325*
LTC_{t-1}	0.044	0.221***	0.401***
XRP_{t-1}	0.018	0.012	0.176***
Observations	303	303	303
Residual Std. Error	3.140	5.783	9.461
R^2	0.081	0.048	0.095
Adjusted R^2	0.072	0.039	0.086
F Statistic	8.769***	5.056***	10.454***

Notes: All the roots are inside the unit circle, and the system is dynamically stable. *, **, and *** indicate statistical significance at the 10%, 5%, and 1% levels respectively.

Table 17: Diagnostic Test Statistics for VAR - Segment 3

		Univariate Tests by Equation:		
Test	Multivariate	BTC	LTC	XRP
$LB_{(1)}$	1.46^{***}	1.12	0.11	0.22
$LB_{(2)}$	19.76^{**}	15.02^{***}	3.02	0.63
$LB_{(3)}$	70.16^{***}	15.11^{***}	3.21	8.04^{**}
$LB_{(4)}$	88.81^{***}	15.12^{***}	3.75	8.60^{*}
$LB_{(5)}$	95.61^{***}	15.23^{***}	3.77	9.12
$LB_{(6)}$	108.51^{***}	16.18^{**}	4.75	12.30^{*}
$LB_{(7)}$	118.36^{***}	16.46^{**}	5.16	12.83^{*}
$LB_{(10)}$	163.64^{***}	18.29^{*}	11.08	31.49^{***}
$ARCH_{(1)}$	160.08^{***}	68.01^{***}	1.15	0.67
$ARCH_{(2)}$	256.03^{***}	79.17^{***}	1.15	12.40^{***}
$ARCH_{(3)}$	500.08^{***}	79.22^{***}	1.58	12.46^{***}
$ARCH_{(4)}$	587.59^{***}	78.87^{***}	1.70	12.41^{**}
$ARCH_{(5)}$	647.00^{***}	83.29^{***}	1.68	12.40^{**}
$ARCH_{(6)}$	689.07^{***}	82.94^{***}	1.71	12.35^{*}
$ARCH_{(7)}$	731.28^{***}	83.72^{***}	3.39	12.35^{*}
$ARCH_{(10)}$	860.78^{***}	86.68^{***}	3.68	12.81
JB	30456.29^{***}	129.05^{***}	3841.57^{***}	22522.17^{***}
Skewness	1673.42^{***}	-0.44^{***}	2.61^{***}	4.57^{***}
Kurtosis	28782.87^{***}	6.07^{***}	19.65^{***}	44.24^{***}

Notes: LB, ARCH, JB, Skewness, and Kurtosis indicate Ljung–Box test for autocorrelation, ARCH test for autoregressive conditional heteroskedasticity, Jarque–Bera test for normality, Skewness test for only skewness, and Kurtosis test for only kurtosis respectively. Values in parenthesis indicate the lag length used in LB and ARCH tests. *, **, and *** indicate statistical significance at the 10%, 5%, and 1% levels respectively.

Table 18: Granger–Causality Test Statistics - Segment 3

	BTC	LTC	XRP
BTC		0.09	2.99^{*}
LTC	1.50		14.00^{***}
XRP	0.92	0.11	

Notes: Value in each cell indicates the test statistics for the hypothesis H_0 that is the row variable does not Granger–cause the column variable. *, **, and *** indicate statistical significance at the 10%, 5%, and 1% levels respectively.

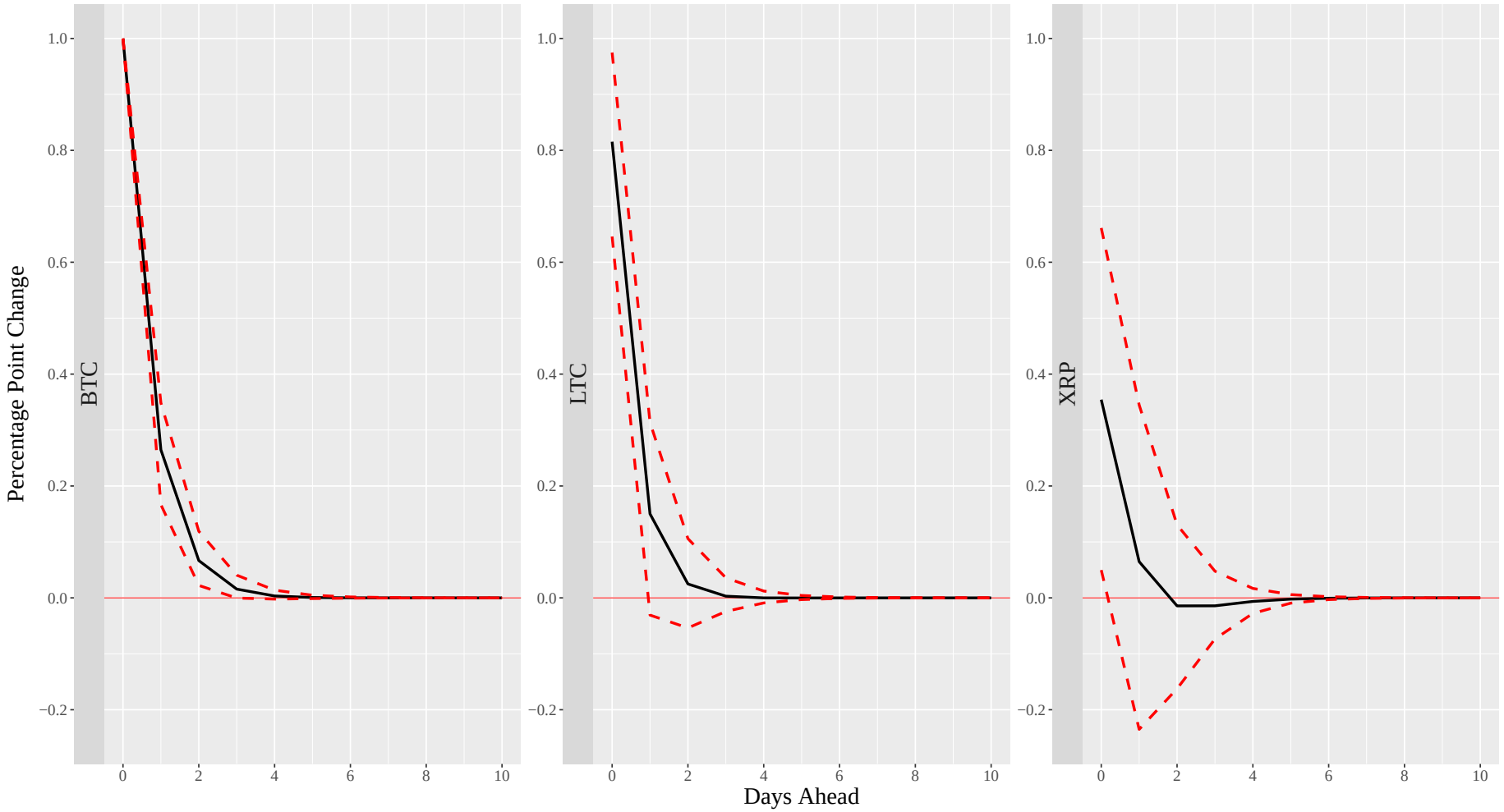

Notes: All variables are in the rate of return form in the estimation, but the interpretation of IRFs is in percentage point change with a 90% confidence interval generated with 10000 bootstrap replications.

(a) Response of All Variables to a One-Percentage-Point Positive Shock in Rate of Return Bitcoin Price - Segment 3

Figure 5: Impulse Responses Analysis - Segment 3

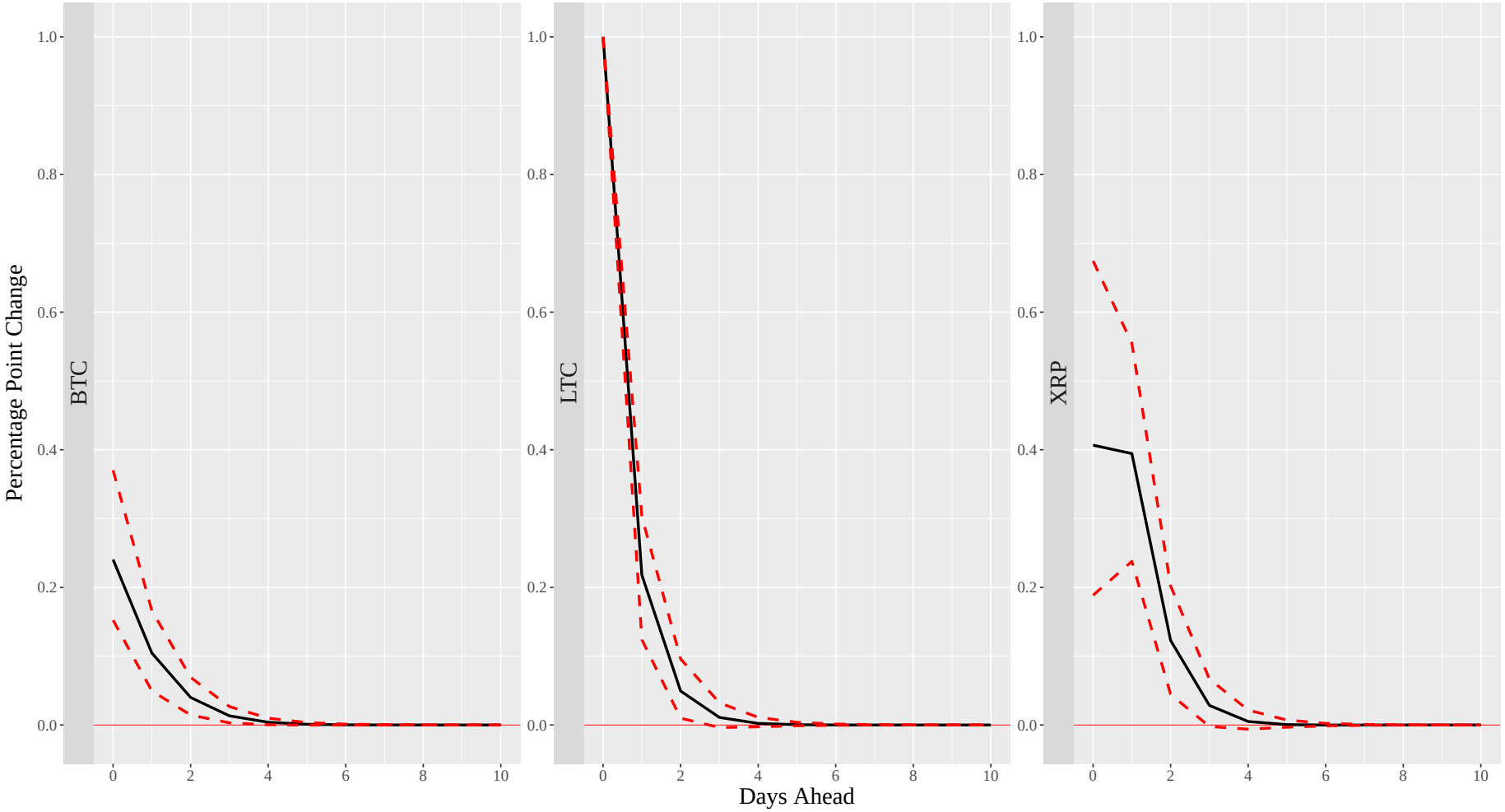

Notes: All variables are in the rate of return form in the estimation, but the interpretation of IRFs is in percentage point change with a 90% confidence interval generated with 10000 bootstrap replications.

(b) Response of All Variables to a One-Percentage-Point Positive Shock in Rate of Return Litecoin Price - Segment 3

Figure 5 (continued)

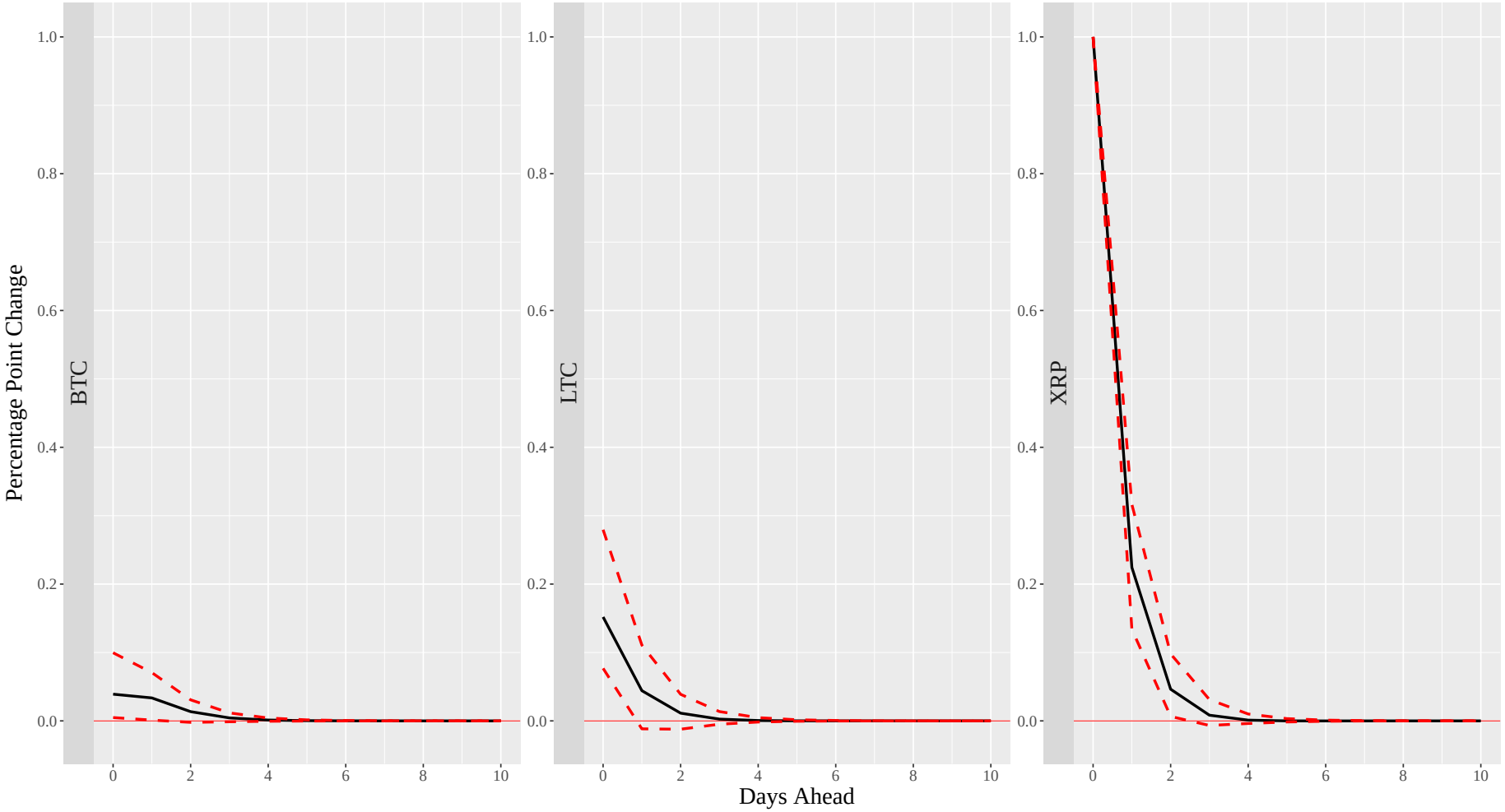

Notes: All variables are in the rate of return form in the estimation, but the interpretation of IRFs is in percentage point change with a 90% confidence interval generated with 10000 bootstrap replications.

(c) Response of All Variables to a One-Percentage-Point Positive Shock in Rate of Return Ripple Price - Segment 3

Figure 5 (continued)

References

Akaike, H. (1974). "A New Look at the Statistical Model Identification". *IEEE Transactions on Automatic Control* 19.6, pp. 716–723.

— (1998). "Information Theory and an Extension of the Maximum Likelihood Principle". *Selected Papers of Hirotugu Akaike*, pp. 199–213.

Bai, J. et al. (2000). *Vector Autoregressive Models with Structural Changes in Regression Coefficients and in Variance-Covariance Matrices*. Tech. rep. China Economics, Management Academy, Central University of Finance, and Economics.

Bai, J., R.L. Lumsdaine, and J.H. Stock (1998). "Testing for and Dating Common Breaks in Multivariate Time Series". *Review of Economic Studies* 65.3, pp. 395–432.

Bai, J. and P. Perron (1998). "Estimating and Testing Linear Models with Multiple Structural Changes". *Econometrica* 66.1, p. 47.

— (2003a). "Computation and Analysis of Multiple Structural Change Models". *Journal of Applied Economics* 18.1, pp. 1–22.

— (2003b). "Critical Values for Multiple Structural Change Tests". *The Econometrics Journal* 6.1, pp. 72–78.

— (2004). "Multiple Structural Change Models: A Simulation Analysis". In: *Frontiers of Analysis and Applied Research*. Ed. by D. Corbae, S.N. Durlauf, and B.E. Hansen. Cambridge University Press (CUP), pp. 212–238.

Bouoiyour, J. and R. Selmi (2015). "What Does Bitcoin Look like?" *Annals of Economics & Finance* 16.2.

— (2016). "Bitcoin: A Beginning of a New Phase". *Economics Bulletin* 36.3, pp. 1430–1440.

BraveNewCoin (2017). *Historical Global Price Indices for Cryptocurrencies*. URL: `https://goo.gl/9JOOrU` (visited on July 30, 2017).

Canova, F. and B.E. Hansen (1995). "Are Seasonal Patterns Constant over Time? A Test for Seasonal Stability". *Journal of Business & Economic Statistics* 13.3, p. 237.

Cheah, E. and J. Fry (2015). "Speculative Bubbles in Bitcoin Markets? An Empirical Investigation into the Fundamental Value of Bitcoin". *Economics Letters* 130, pp. 32–36.

Chuen, D.L.K. (2015). *Handbook of Digital Currency: Bitcoin, Innovation, Financial Instruments, and Big Data*. Academic Press.

Ciaian, P., M. Rajcaniova, and D. Kancs (2015). "The Economics of Bitcoin Price Formation". *Applied Economics* 48.19, pp. 1799–1815.

CoinMarketCap (2017a). *CryptoCurrency Historical Weekly Snapshots*. URL: `https://goo.gl/v1dFCi` (visited on July 30, 2017).

— (2017b). *CryptoCurrency Market Capitalizations*. URL: `https://goo.gl/wjR9sH` (visited on July 30, 2017).

CoinMarketCap (2017c). *CryptoCurrency Monthly Volume Rankings in USD*. URL: https://goo.gl/i7q2Vk (visited on July 30, 2017).

Dickey, D.A. and W.A. Fuller (1979). "Distribution of the Estimators for Autoregressive Time Series with a Unit Root". *Journal of the American Statistical Association* 74.366a, pp. 427–431.

— (1981). "Likelihood Ratio Statistics for Autoregressive Time Series with a Unit Root". *Econometrica* 49.4, p. 1057.

Elliott, G., T.J. Rothenberg, and J.H. Stock (1996). "Efficient Tests for an Autoregressive Unit Root". *Econometrica* 64.4, p. 813.

Enders, W. (2004). "Applied Econometric Time Series, by Walter". *Technometrics* 46.2, p. 264.

Engle, R.F. (1982). "Autoregressive Conditional Heteroscedasticity with Estimates of the Variance of United Kingdom Inflation". *Econometrica* 50.4, p. 987.

Fink, C. and T. Johann (2014). "Bitcoin Markets".

Georgoula, I., D. Pournarakis, C. Bilanakos, D.N. Sotiropoulos, and G.M. Giaglis (2015). "Using Time-Series and Sentiment Analysis to Detect the Determinants of Bitcoin Prices". *SSRN Electronic Journal*.

Granger, C.W.J. (1969). "Investigating Causal Relations by Econometric Models and Cross-Spectral Methods". *Econometrica* 37.3, p. 424.

Granger, C.W.J. and P. Newbold (1974). "Spurious Regressions in Econometrics". *Journal of Econometrics* 2.2, pp. 111–120.

Hamilton, J.D. (1994). *Time Series Analysis*. Vol. 2. Princeton university press Princeton.

Hosking, J.R. (1980). "The Multivariate Portmanteau Statistic". *Journal of the American Statistical Association* 75.371, pp. 602–608.

— (1981). "Lagrange-Multiplier Tests of Multivariate Time-Series Models". *Journal of the Royal Statistical Society. Series B (Methodological)*, pp. 219–230.

Hyndman, R.J. and G. Athanasopoulos (2014). *Forecasting: Principles and Practice*. OTexts.

Jarque, C.M. and A.K. Bera (1987). "A Test for Normality of Observations and Regression Residuals". *International Statistical Review* 55.2, p. 163.

Koop, G., M.H. Pesaran, and S.M. Potter (1996). "Impulse Response Analysis in Nonlinear Multivariate Models". *Journal of Econometrics* 74.1, pp. 119–147.

Kristoufek, L. (2015). "What Are the Main Drivers of the Bitcoin Price? Evidence from Wavelet Coherence Analysis". *PLOS ONE* 10.4. Ed. by E. Scalas, e0123923.

Kwiatkowski, D., P.C.B. Phillips, P. Schmidt, and Y. Shin (1992). "Testing the Null Hypothesis of Stationarity against the Alternative of a Unit Root: How Sure Are We that Economic Time Series Have a Unit Root?" *Journal of Econometrics* 54.1, pp. 159–178.

Li, W. and A. Mcleod (1981). “Distribution of the Residual Autocorrelations in Multivariate ARMA Time Series Models”. *Journal of the Royal Statistical Society. Series B (Methodological)*, pp. 231–239.

Li, X. and C.A. Wang (2017). “The Technology and Economic Determinants of Cryptocurrency Exchange Rates: The Case of Bitcoin”. *Decision Support Systems* 95, pp. 49–60.

Ljung, G.M. and G.E.P. Box (1978). “On a Measure of Lack of Fit in Time Series Models”. *Biometrika* 65.2, pp. 297–303.

Lütkepohl, H. (2005). *New Introduction to Multiple Time Series Analysis*. Springer Science & Business Media.

— (2006). “Structural Vector Autoregressive Analysis for Cointegrated Variables”. In: *Modern Econometric Analysis*. Springer, pp. 73–86.

— (2011). *Vector Autoregressive Models*. Springer.

Lütkepohl, H. and H. Reimers (1992). “Impulse Response Analysis of Cointegrated Systems”. *Journal of Economic Dynamics & Control* 16.1, pp. 53–78.

Malhotra, A. and M. Maloo (2014). “Bitcoin is it a Bubble? Evidence from Unit Root Tests”. *SSRN Electronic Journal*.

Nakamoto, S. (2008). “Bitcoin: A Peer-to-Peer Electronic Cash System”. *Consulted* 1.2012, p. 28.

Ng, S. and P. Perron (2001). “Lag Length Selection and the Construction of Unit Root Tests with Good Size and Power”. *Econometrica* 69.6, pp. 1519–1554.

Osborn, D.R., A.P.L. Chui, J.P. Smith, and C.R. Birchenhall (1988). “Seasonality and the Order of Integration for Consumption”. *Oxford Bulletin of Economics and Statistics* 50.4, pp. 361–377.

Osterrieder, J., M. Strika, and J. Lorenz (2017). “Bitcoin and Cryptocurrencies—not for the Faint-Hearted”. *International Finance and Banking* 4.1, p. 56.

Perron, P. (1997). “Further Evidence on Breaking Trend Functions in Macroeconomic Variables”. *Journal of Econometrics* 80.2, pp. 355–385.

— (2006). “Dealing with Structural Breaks”. *Palgrave Handbook of Econometrics* 1, pp. 278–352.

Perron, P. and Z. Qu (2006). “Estimating Restricted Structural Change Models”. *Journal of Econometrics* 134.2, pp. 373–399.

Phillips, P.C.B. (1986). “Understanding Spurious Regressions in Econometrics”. *Journal of Econometrics* 33.3, pp. 311–340.

Phillips, P.C.B. and P. Perron (1988). “Testing for a Unit Root in Time Series Regression”. *Biometrika* 75.2, pp. 335–346.

Qu, Z. and P. Perron (2007). "Estimating and Testing Structural Changes in Multivariate Regressions". *Econometrica* 75.2, pp. 459–502.

Quandl (2017). *BNC Digital Currency Indexed EOD*. URL: `https://goo.gl/BVpCJe` (visited on July 30, 2017).

Rissanen, J. (1978). "Modeling by Shortest Data Description". *Automatica* 14.5, pp. 465–471.

Schwarz, G. et al. (1978). "Estimating the Dimension of a Model". *The Annals of Statistics* 6.2, pp. 461–464.

Schwert, G.W. (1989). "Tests for Unit Roots: A Monte Carlo Investigation". *Journal of Business & Economic Statistics*, pp. 147–159.

Sims, C.A. (1980). "Macroeconomics and Reality". *Econometrica: Journal of the Econometric Society*, pp. 1–48.

Tsay, R.S. (2005). *Analysis of Financial Time Series*. Vol. 543. John Wiley &; Sons.

Wang, J., Y. Xue, and M. Liu (2016). "An Analysis of Bitcoin Price Based on VEC Model". In: *Proceedings of the 2016 International Conference on Economics and Management Innovations*. Atlantis Press.

Watson, M.W. (1994). "Vector Autoregressions and Cointegration". *Handbook of Econometrics* 4, pp. 2843–2915.

Zhu, Y., D. Dickinson, and J. Li (2017). "Analysis on the Influence Factors of Bitcoin's Price Based on Vec Model". *Financial Innovation* 3.1, p. 3.

Appendix

A R Version Information

- R version 3.3.3 (2017-03-06), `x86_64-apple-darwin13.4.0`
- Locale: `en_US.UTF-8/en_US.UTF-8/en_US.UTF-8/C/en_US.UTF-8/en_US.UTF-8`
- Base packages: base, datasets, graphics, grDevices, grid, methods, stats, utils
- Other packages: aod 1.3, bestglm 0.36, bitops 1.0-6, boot 1.3-20, CADFtest 0.3-3, car 2.1-6, checkpoint 0.4.3, classInt 0.1-24, cowplot 0.9.2, devtools 1.13.4, downloader 0.4, dplyr 0.7.4, dygraphs 1.1.1.4, dynlm 0.3-5, fBasics 3042.89, FitAR 1.94, forecast 8.2, Formula 1.2-2, fUnitRoots 3042.79, ggplot2 2.2.1.9000, ggthemes 3.4.0, gridExtra 2.3, gtable 0.2.0, gvlma 1.0.0.2, Hmisc 4.1-1, knitr 1.19, latex2exp 0.4.0, lattice 0.20-35, latticeExtra 0.6-28, leaps 3.0, lgarch 0.6-2, lmtest 0.9-35, ltsa 1.4.6, lubridate 1.7.1, magrittr 1.5, MASS 7.3-47, moments 0.14, NCmisc 1.1.5, NLP 0.1-11, normtest 1.1, nortest 1.0-4, pastecs 1.3-18, plyr 1.8.4, Quandl 2.9.0, RColorBrewer 1.1-2, RCurl 1.95-4.10, reshape 0.8.7, reshape2 1.4.3, rvest 0.3.2, sandwich 2.4-0, scales 0.5.0.9000, seasonal 1.6.1, sp 1.2-6, stargazer 5.2.1, stringi 1.1.6, stringr 1.2.0, strucchange 1.5-1, survival 2.41-3, tidyr 0.7.2, tikzDevice 0.10-1, timeDate 3042.101, timeSeries 3042.102, tm 0.7-3, tsDyn 0.9-44, tseries 0.10-42, urca 1.3-0, vars 1.5-2, x13binary 1.1.39-1, XLConnect 0.2-14, XLConnectJars 0.2-14, xml2 1.1.1, xtable 1.8-2, xts 0.10-1, zoo 1.8-1
- Loaded via a namespace (and not attached): acepack 1.4.1, assertthat 0.2.0, backports 1.1.2, base64enc 0.1-3, bindr 0.1, bindrcpp 0.2, checkmate 1.8.5, class 7.3-14, cluster 2.0.6, codetools 0.2-15, colorspace 1.3-2, curl 3.1, data.table 1.10.4-3, digest 0.6.15, e1071 1.6-8, filehash 2.4-1, foreach 1.4.4, foreign 0.8-69, fracdiff 1.4-2, glmnet 2.0-13, glue 1.2.0, grpreg 3.1-2, htmlTable 1.11.2, htmltools 0.3.6, htmlwidgets 1.0, httr 1.3.1, iterators 1.0.9, jsonlite 1.5, lazyeval 0.2.1, lme4 1.1-15, Matrix 1.2-11, MatrixModels 0.4-1, memoise 1.1.0, mgcv 1.8-22, minqa 1.2.4, mnormt 1.5-5, munsell 0.4.3, nlme 3.1-131, nloptr 1.0.4, nnet 7.3-12, parallel 3.3.3, pbkrtest 0.4-7, pkgconfig 2.0.1, proftools 0.99-2, purrr 0.2.4, quadprog 1.5-5, quantmod 0.4-12, quantreg 5.34, R6 2.2.2, Rcpp 0.12.14, rJava 0.9-9, rlang 0.1.6, rpart 4.1-11, rstudioapi 0.7, slam 0.1-40, SparseM 1.77, spatial 7.3-11, splines 3.3.3, tibble 1.3.4, tools 3.3.3, tseriesChaos 0.1-13, TTR 0.23-2, withr 2.1.1, yaml 2.1.16

B GAUSS Version Information

GAUSS software used in this study is version 16.04 build 4222.

C Additional Tables and Figures

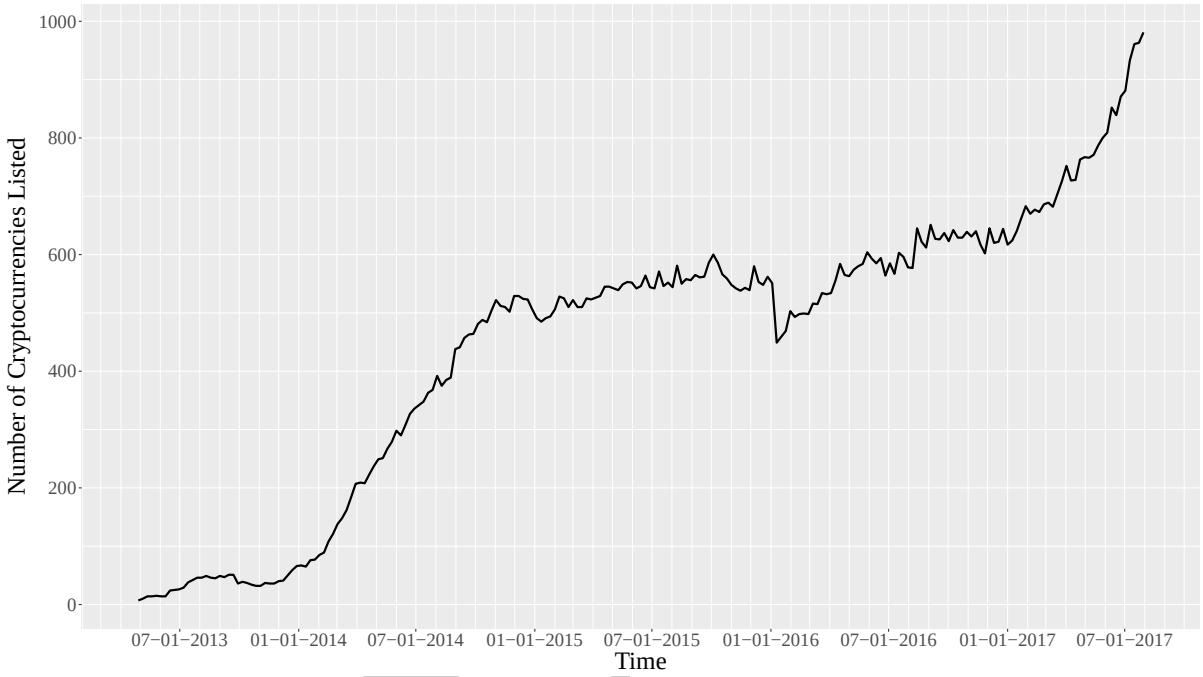

Figure 6: Number of Cryptocurrencies Listed

Note: Based on weekly snapshots from April 28, 2013 to July 30, 2017 (CoinMarketCap, 2017a).

Table 19: Top Cryptocurrencies by Market Capitalization

#	Cryptocurrency	Symbol	Market Cap.	Price	Circulating Supply	Volume(24h)	% Market Cap.	% Volume(24h)
1	Bitcoin	BTC	$45,142,382,113	$2,739.43	16,478,750	$723,314,000	50.43	36.20
2	Ethereum	ETH	$18,901,688,291	$201.79	93,670,558	$774,864,000	21.12	38.78
3	Ripple	XRP	$6,385,947,908	$0.17	38,333,090,674	$58,993,700	7.13	2.95
4	Litecoin	LTC	$2,140,008,002	$40.96	52,240,932	$87,295,000	2.39	4.37
5	NEM	XEM	$1,497,978,000	$0.17	8,999,999,999	$2,272,910	1.67	0.11
6	Ethereum Classic	ETC	$1,317,774,969	$14.01	94,057,584	$43,468,200	1.47	2.18
7	Dash	DASH	$1,316,414,649	$176.52	7,457,679	$27,246,600	1.47	1.36
8	IOTA	MIOTA	$732,914,884	$0.26	2,779,530,283	$3,213,680	0.82	0.16
9	Monero	XMR	$610,276,308	$41.06	14,861,481	$10,543,600	0.68	0.53
10	Stratis	STRAT	$484,611,812	$4.92	98,483,723	$10,166,600	0.54	0.51
11	EOS	EOS	$448,698,302	$1.78	251,649,328	$30,716,300	0.50	1.54
12	BitConnect	BCC	$391,419,688	$62.10	6,303,471	$2,246,190	0.44	0.11
13	NEO	ANS	$359,661,000	$7.19	50,000,000	$9,552,000	0.40	0.48
14	Zcash	ZEC	$333,150,840	$179.75	1,853,381	$17,460,700	0.37	0.87
15	BitShares	BTS	$331,719,278	$0.13	2,597,340,000	$21,350,400	0.37	1.07
16	Qtum	QTUM	$330,167,540	$5.60	59,000,000	$3,721,790	0.37	0.19
17	Tether	USDT	$319,919,759	$1.00	319,501,213	$68,103,400	0.36	3.41
18	Veritaseum	VERI	$296,991,550	$148.03	2,006,279	$583,892	0.33	0.03
19	Steem	STEEM	$295,569,011	$1.24	238,312,137	$847,769	0.33	0.04
20	Waves	WAVES	$287,822,000	$2.88	100,000,000	$1,705,820	0.32	0.09

Notes: Downloaded on July 30, 2017 19:25 UTC from CoinMarketCap (2017b). All monetary values are in nominal prices.

Table 20: Top Cryptocurrencies by Monthly Volume

#	Cryptocurrency	Symbol	Volume(1d)	Volume(7d)	Volume(30d)	% Volume(1d)	% Volume(7d)	% Volume(30d)
1	Bitcoin	BTC	$732,328,000	$5,996,735,936	$30,812,284,864	35.78	40.69	31.64
2	Ethereum	ETH	$804,847,000	$4,140,150,592	$29,369,701,888	39.33	28.09	30.16
3	Litecoin	LTC	$88,956,400	$738,573,736	$10,253,069,960	4.35	5.01	10.53
4	Ethereum Classic	ETC	$44,472,100	$275,607,652	$4,240,702,180	2.17	1.87	4.35
5	Ripple	XRP	$60,836,900	$468,203,406	$3,661,316,034	2.97	3.18	3.76
6	Tether	USDT	$69,395,600	$665,443,864	$3,550,181,728	3.39	4.52	3.65
7	EOS	EOS	$31,162,100	$288,444,644	$2,785,866,732	1.52	1.96	2.86
8	BitShares	BTS	$21,765,300	$321,618,252	$1,800,496,348	1.06	2.18	1.85
9	Dash	DASH	$27,640,300	$248,231,670	$1,329,233,470	1.35	1.68	1.36
10	Zcash	ZEC	$17,774,600	$120,363,746	$676,787,265	0.87	0.82	0.69
11	Status	SNT	$10,042,500	$172,151,612	$598,315,157	0.49	1.17	0.61
12	NEO	ANS	$9,801,840	$86,537,825	$562,275,387	0.48	0.59	0.58
13	FirstBlood	1ST	$1,279,340	$20,419,337	$450,306,921	0.06	0.14	0.46
14	Qtum	QTUM	$3,816,580	$69,966,440	$403,635,741	0.19	0.47	0.41
15	Monero	XMR	$10,534,800	$91,613,111	$392,988,265	0.51	0.62	0.40
16	Siacoin	SC	$4,618,670	$48,851,413	$337,054,412	0.23	0.33	0.35
17	Stratis	STRAT	$10,598,700	$77,749,575	$332,690,901	0.52	0.53	0.34
18	Stellar Lumens	XLM	$3,927,890	$41,122,671	$307,961,304	0.19	0.28	0.32
19	GXShares	GXS	$1,628,640	$34,253,032	$290,289,067	0.08	0.23	0.30
20	DigiByte	DGB	$8,959,530	$77,862,286	$262,422,963	0.44	0.53	0.27

Notes: Downloaded on July 30, 2017 19:17 UTC from CoinMarketCap (2017c). All monetary values are in nominal prices.

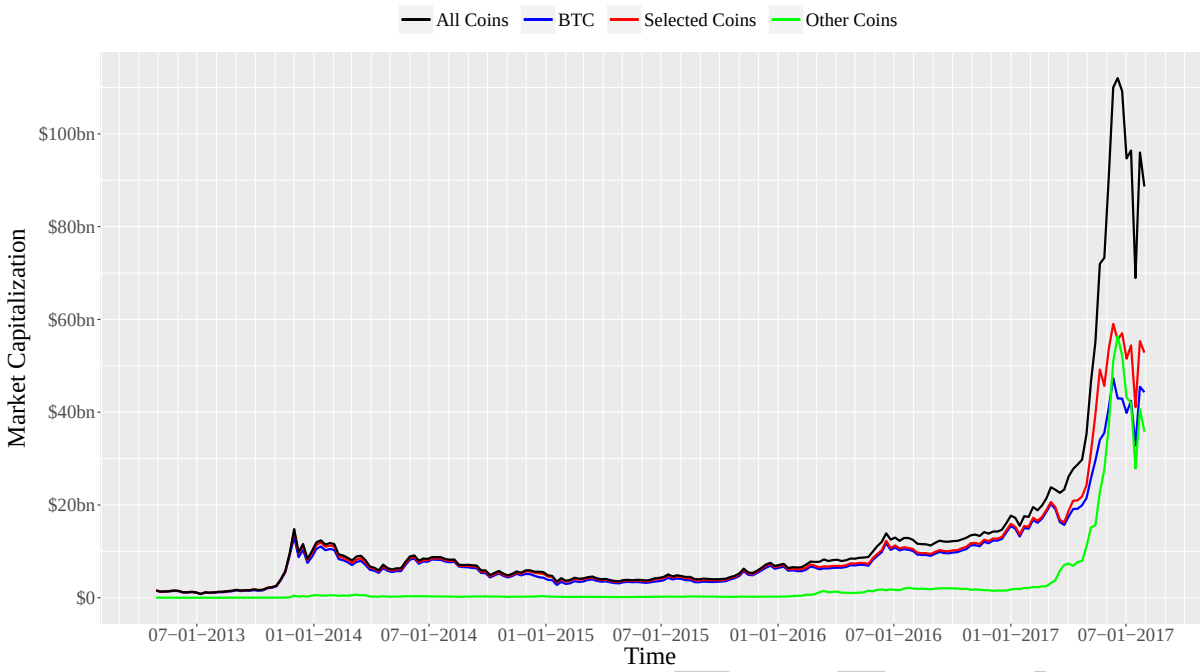

(a) All Coins, Bitcoin, Selected Coins and Other Coins

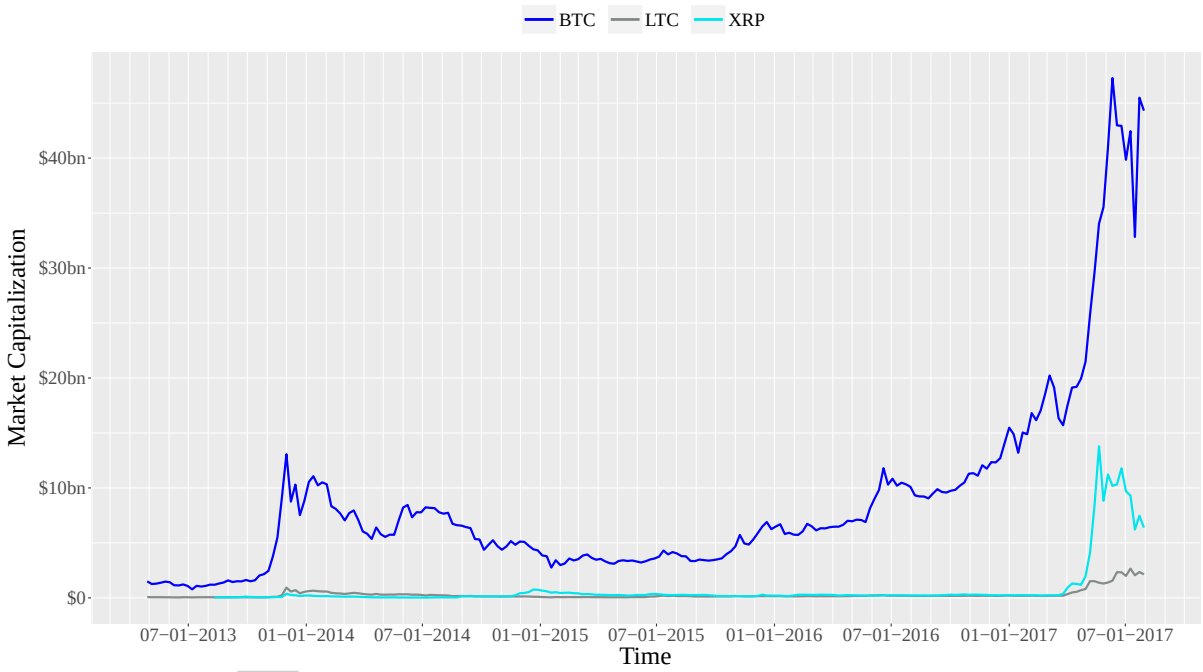

(b) Selected Coins

Figure 7: Market Capitalization by Cryptocurrency

Note: Based on nominal weekly prices from April 28, 2013 to July 30, 2017 (CoinMarketCap, 2017a).

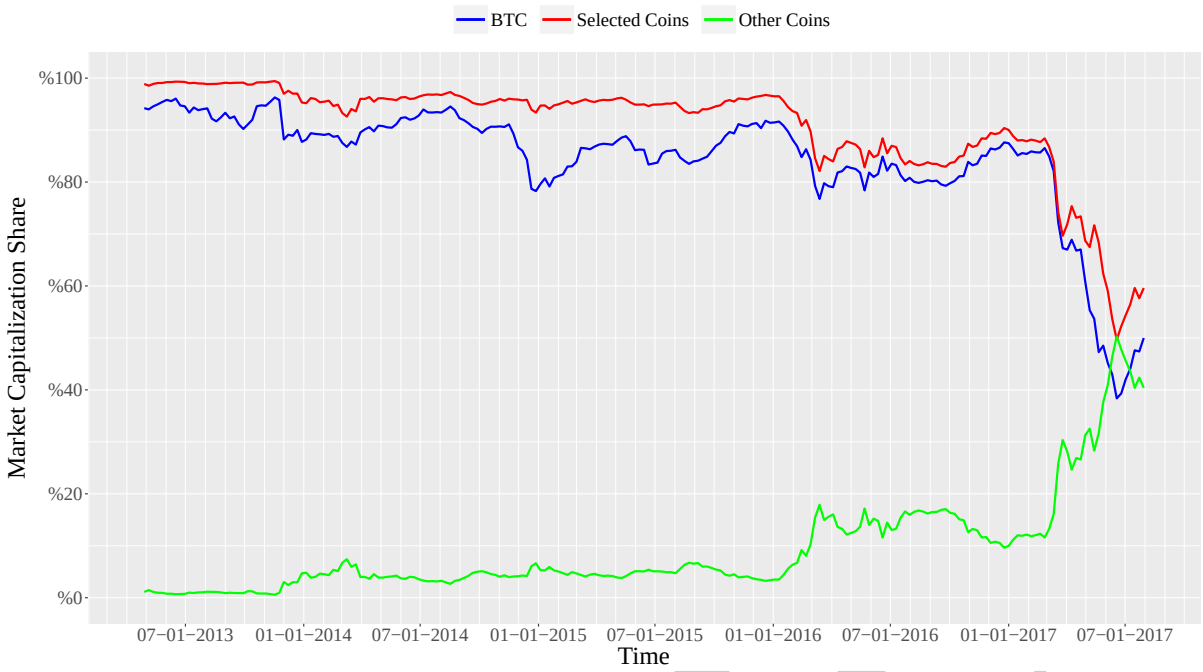

(a) Bitcoin, Selected Coins and Other Coins

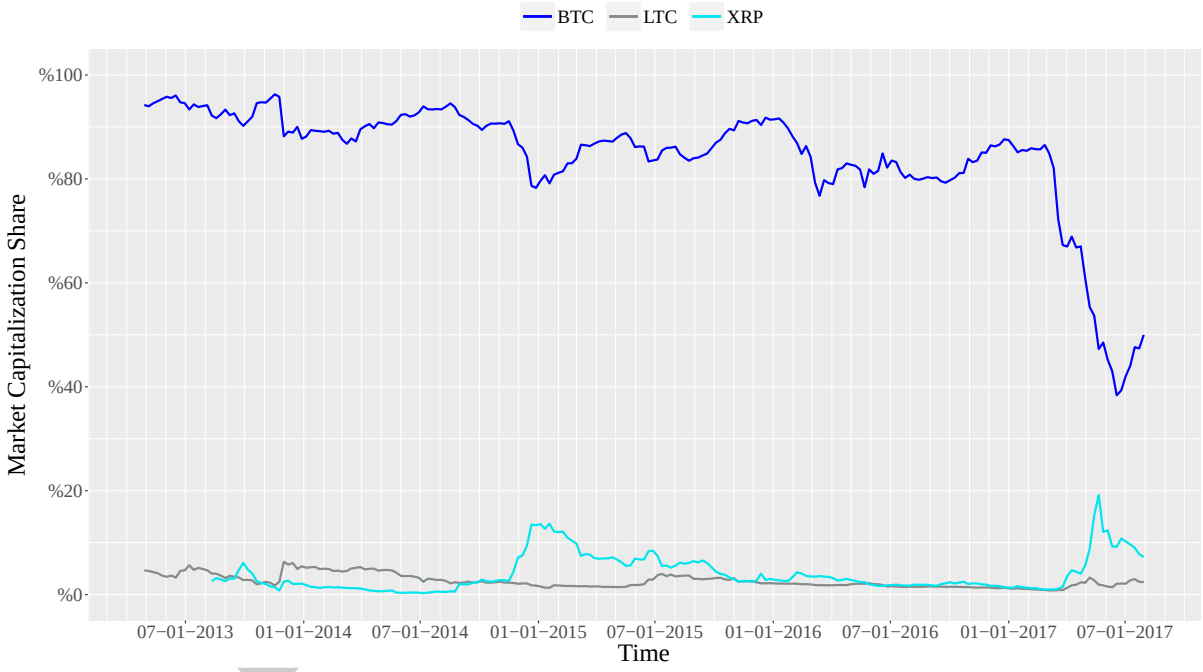

(b) Bitcoin vs. Selected Coins

Figure 8: Market Capitalization Share by Cryptocurrency

Note: Based on nominal weekly prices from April 28, 2013 to July 30, 2017 (CoinMarketCap, 2017a).

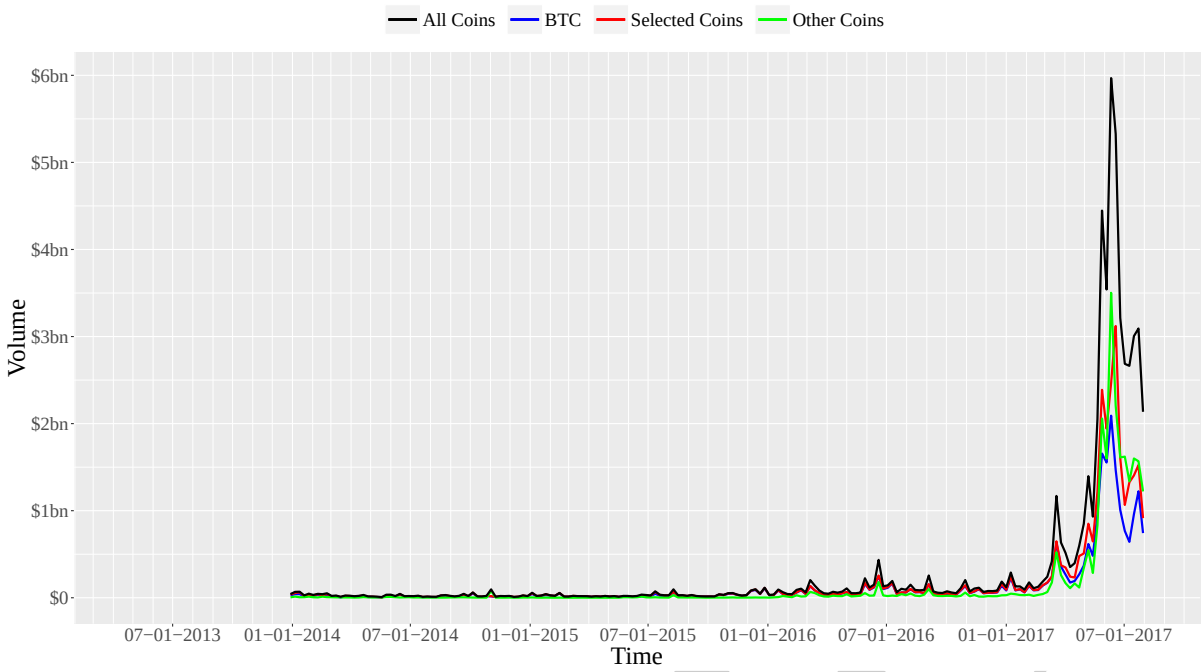

(a) All Coins, Bitcoin, Selected Coins and Other Coins

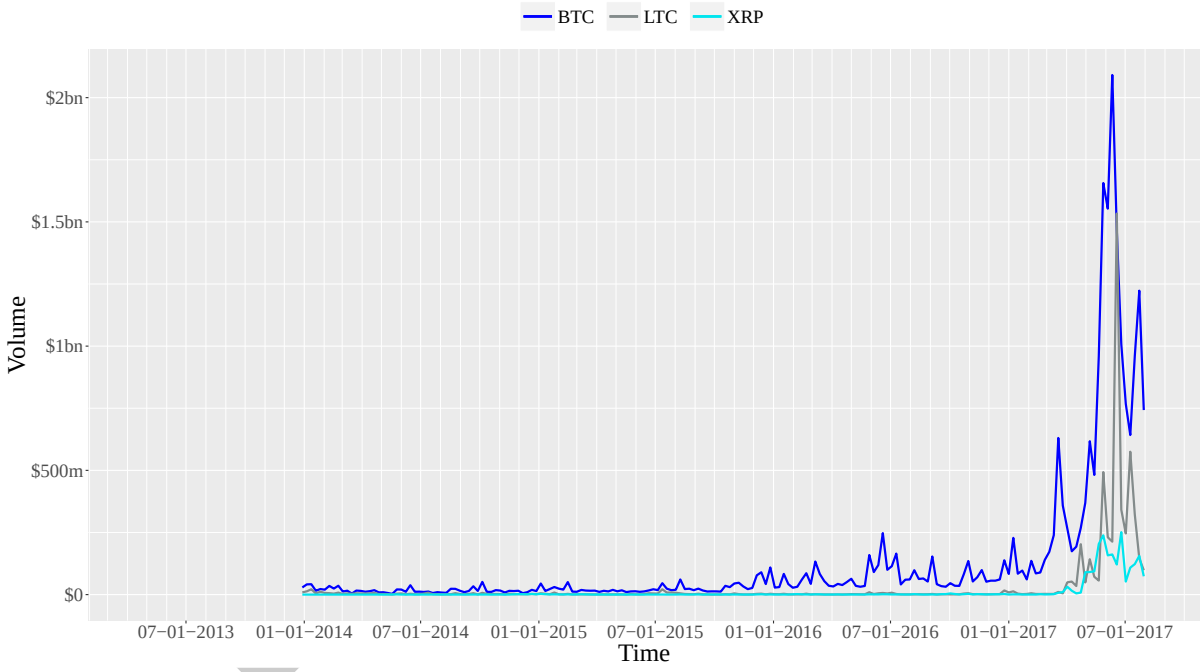

(b) Selected Coins

Figure 9: Volume by Cryptocurrency

Note: Based on nominal weekly prices from April 28, 2013 to July 30, 2017 (CoinMarketCap, 2017a).

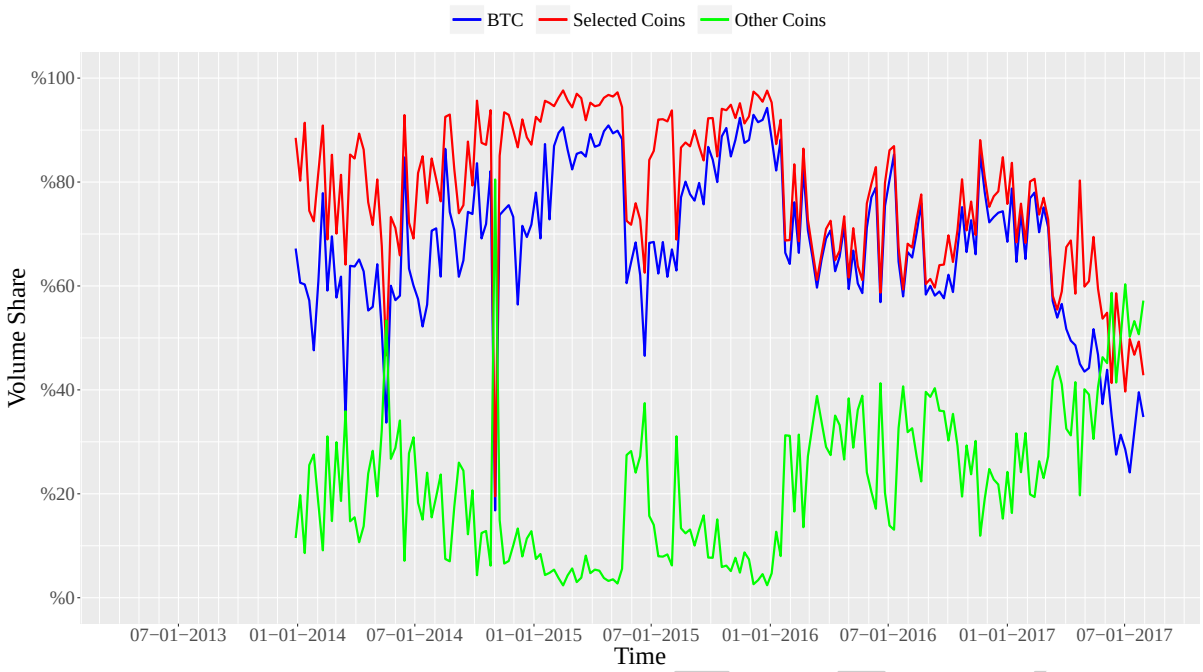

(a) Bitcoin, Selected Coins and Other Coins

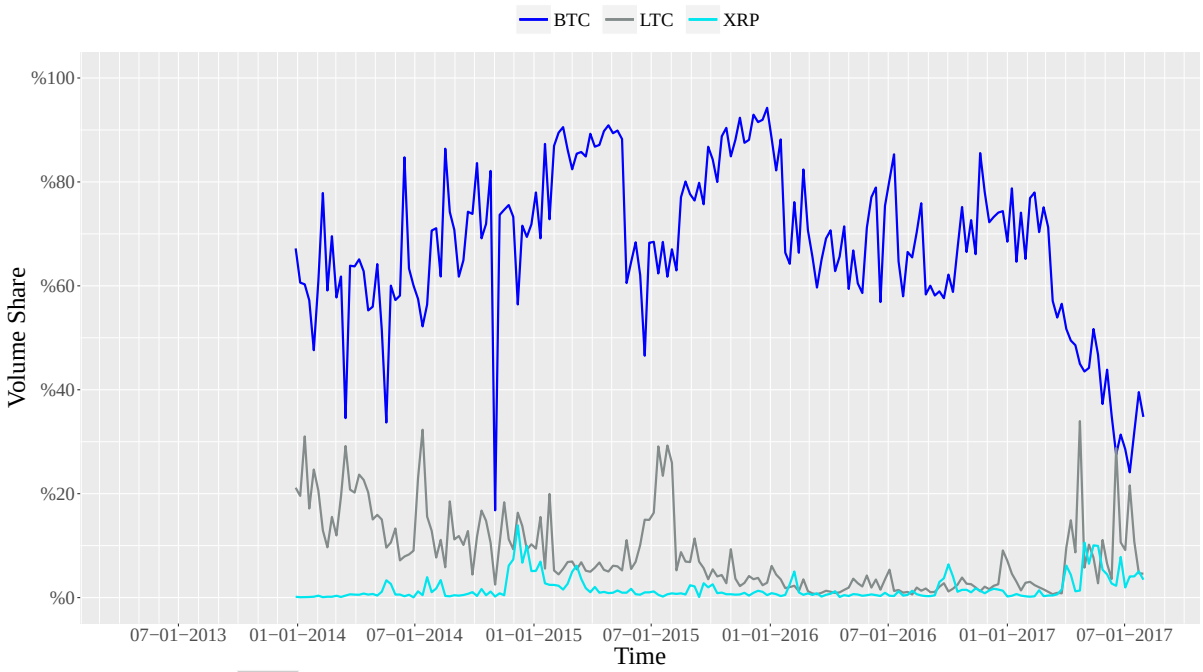

(b) Selected Coins

Figure 10: Volume Share by Cryptocurrency

Note: Based on nominal weekly prices from April 28, 2013 to July 30, 2017 (CoinMarketCap, 2017a).

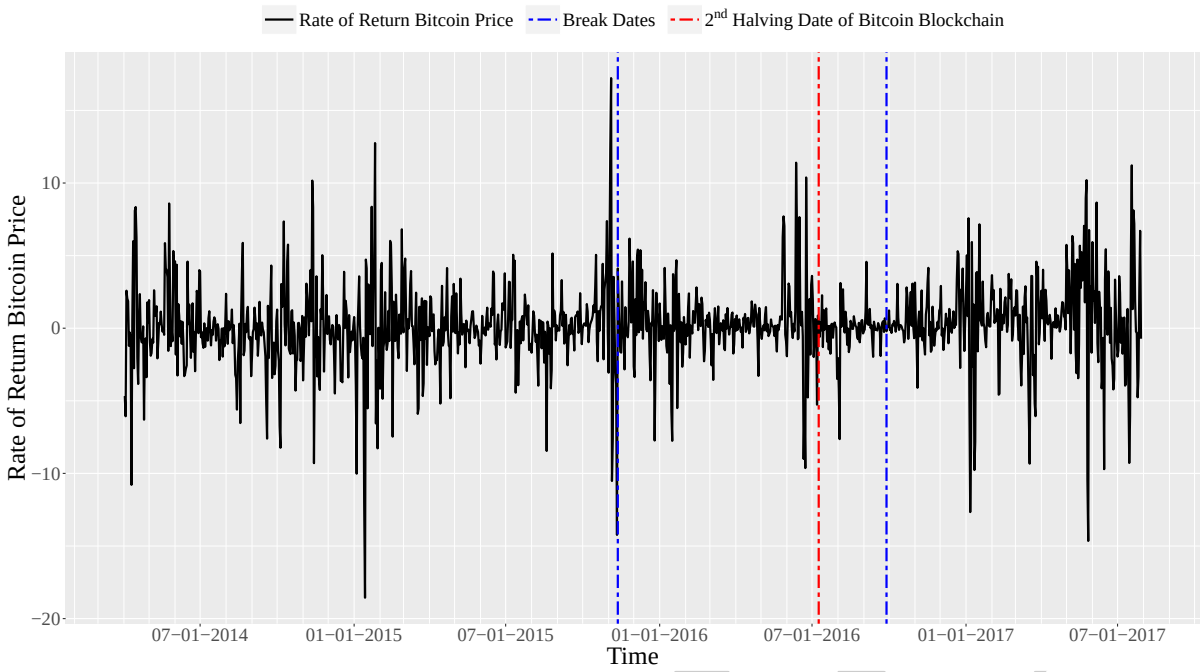

(a) Rate of Return Bitcoin Price

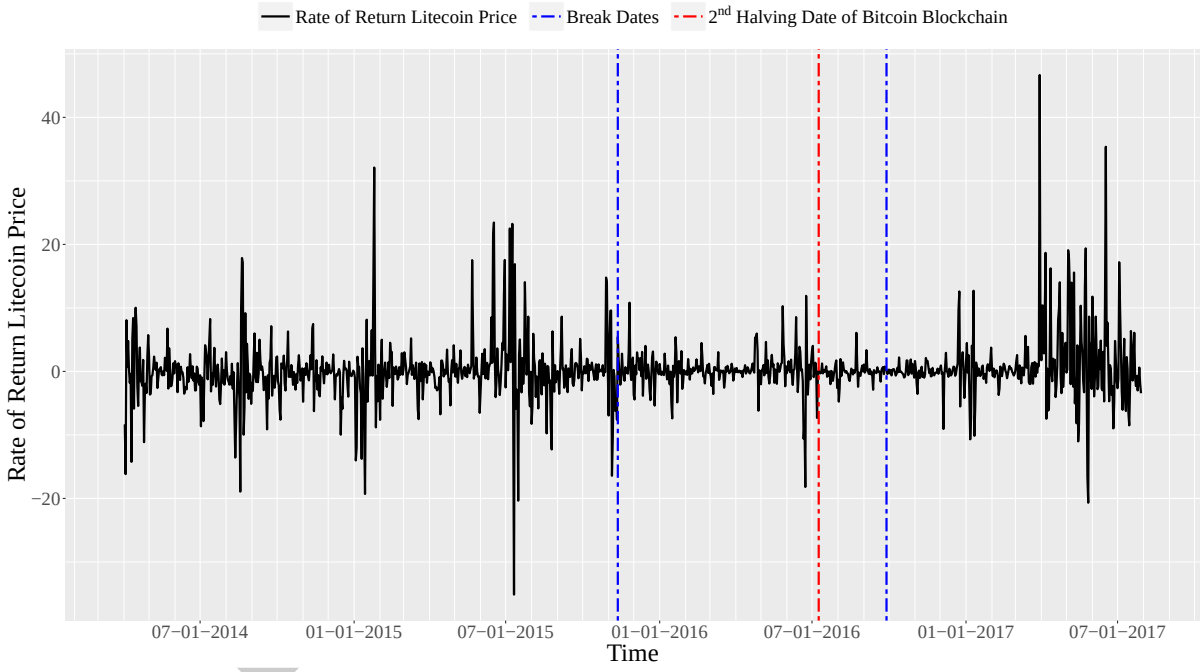

(b) Rate of Return Litecoin Price

Figure 11: Plots of All Variables in Rate of Return Form

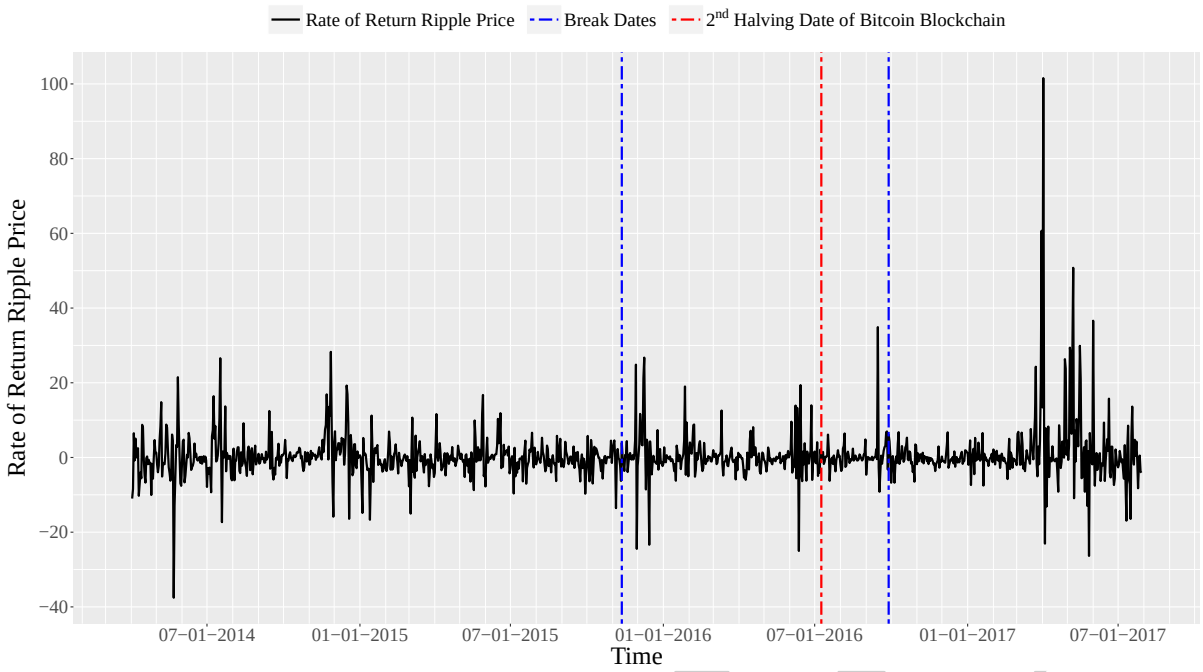

(c) Rate of Return Ripple Price

Figure 11 (continued)

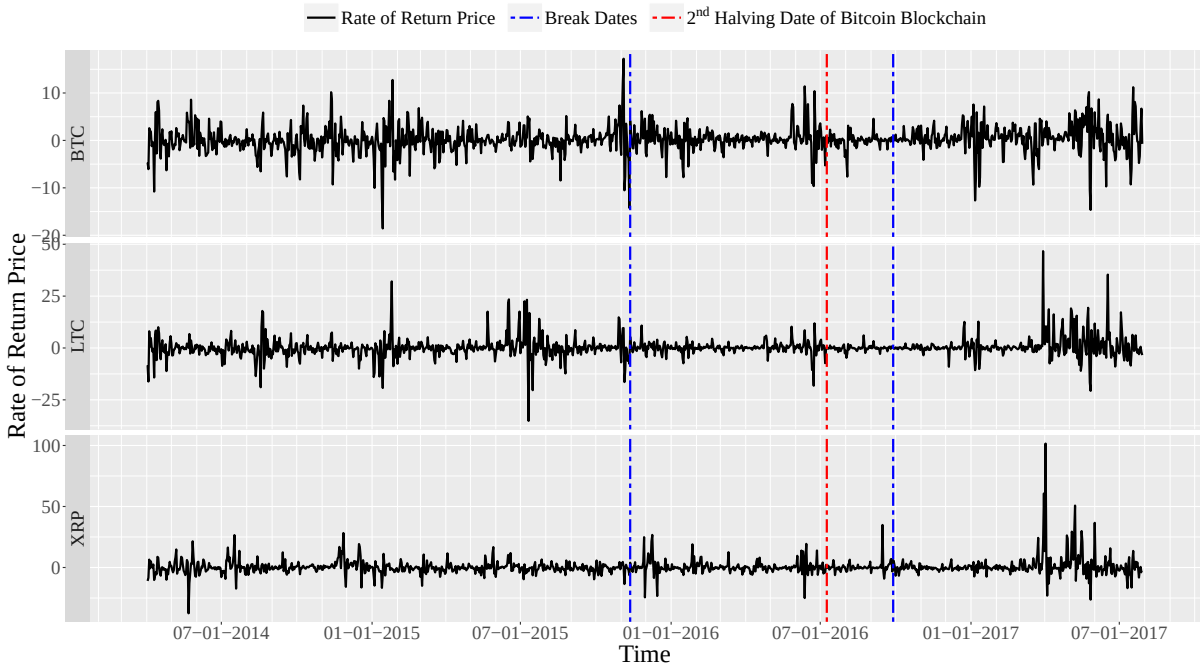

Figure 12: Plots of All Variables Together in Rate of Return Form